

Bates College

SCARAB

---

All Faculty Scholarship

Departments and Programs

---

3-2024

## Borrelia burgdorferi PlzA is a cyclic-di-GMP dependent DNA and RNA binding protein

Nerina Jusufovic

*University of Kentucky College of Medicine*

Andrew C. Krusenstjerna

*University of Kentucky College of Medicine*

Christina R. Savage

*University of Kentucky College of Medicine*

Timothy C. Saylor

*University of Kentucky College of Medicine*

Catherine A. Brissette

*School of Medicine & Health Sciences*

*See next page for additional authors*

Follow this and additional works at: [https://scarab.bates.edu/faculty\\_publications](https://scarab.bates.edu/faculty_publications)

---

### Recommended Citation

Jusufovic, N., Krusenstjerna, A. C., Savage, C. R., Saylor, T. C., Brissette, C. A., Zückert, W. R., Schlax, P. J., Motaleb, M. A., & Stevenson, B. (2024). Borrelia burgdorferi PlzA is a cyclic-di-GMP dependent DNA and RNA binding protein. *Molecular Microbiology*. <https://doi.org/10.1111/mmi.15254>

This Article is brought to you for free and open access by the Departments and Programs at SCARAB. It has been accepted for inclusion in All Faculty Scholarship by an authorized administrator of SCARAB. For more information, please contact [batesscarab@bates.edu](mailto:batesscarab@bates.edu).

---

**Authors**

Nerina Jusufovic, Andrew C. Krusenstjerna, Christina R. Savage, Timothy C. Saylor, Catherine A. Brissette, Wolfram R. Zückert, Paula Schlax, Md A. Motaleb, and Brian Stevenson

# *Borrelia burgdorferi* PlzA is a cyclic-di-GMP dependent DNA and RNA binding protein

Nerina Jusufovic<sup>1</sup> | Andrew C. Krusenstjerna<sup>1</sup> | Christina R. Savage<sup>1</sup> | Timothy C. Saylor<sup>1</sup> | Catherine A. Brissette<sup>2</sup> | Wolfram R. Zückert<sup>3</sup> | Paula J. Schlax<sup>4</sup> | Md A. Motaleb<sup>5</sup> | Brian Stevenson<sup>1,6</sup>

<sup>1</sup>Microbiology, Immunology and Molecular Genetics, University of Kentucky College of Medicine, University of Kentucky, Lexington, Kentucky, USA

<sup>2</sup>Department of Biomedical Sciences, University of North Dakota, School of Medicine and Health Sciences, Grand Forks, North Dakota, USA

<sup>3</sup>Department of Microbiology, Molecular Genetics and Immunology, University of Kansas School of Medicine, Kansas City, Kansas, USA

<sup>4</sup>Department of Chemistry and Biochemistry, Bates College, Lewiston, Maine, USA

<sup>5</sup>Department of Microbiology and Immunology, Brody School of Medicine, East Carolina University, Greenville, North Carolina, USA

<sup>6</sup>Department of Entomology, University of Kentucky, Lexington, Kentucky, USA

## Correspondence

Brian Stevenson, Microbiology, Immunology and Molecular Genetics, University of Kentucky College of Medicine, University of Kentucky, Lexington, KY 40526-0001, USA. Email: [brian.stevenson@uky.edu](mailto:brian.stevenson@uky.edu)

## Funding information

National Institutes of Health, Grant/Award Number: R01 AI144126-3

## Abstract

The PilZ domain-containing protein, PlzA, is the only known cyclic di-GMP binding protein encoded by all Lyme disease spirochetes. PlzA has been implicated in the regulation of many borrelial processes, but the effector mechanism of PlzA was not previously known. Here, we report that PlzA can bind DNA and RNA and that nucleic acid binding requires c-di-GMP, with the affinity of PlzA for nucleic acids increasing as concentrations of c-di-GMP were increased. A mutant PlzA that is incapable of binding c-di-GMP did not bind to any tested nucleic acids. We also determined that PlzA interacts predominantly with the major groove of DNA and that sequence length and G–C content play a role in DNA binding affinity. PlzA is a dual-domain protein with a PilZ-like N-terminal domain linked to a canonical C-terminal PilZ domain. Dissection of the domains demonstrated that the separated N-terminal domain bound nucleic acids independently of c-di-GMP. The C-terminal domain, which includes the c-di-GMP binding motifs, did not bind nucleic acids under any tested conditions. Our data are supported by computational docking, which predicts that c-di-GMP binding at the C-terminal domain stabilizes the overall protein structure and facilitates PlzA-DNA interactions via residues in the N-terminal domain. Based on our data, we propose that levels of c-di-GMP during the various stages of the enzootic life cycle direct PlzA binding to regulatory targets.

## KEYWORDS

*Borrelia*, cyclic-di-GMP, DNA-binding protein, Lyme disease

## 1 | INTRODUCTION

Cyclic bis-(3' → 5')-dimeric guanosine monophosphate (c-di-GMP) is a ubiquitous bacterial cyclic di-nucleotide. In many bacterial species, it engages in the regulation of key processes such as transcription,

motility, biofilm formation, and virulence (Hengge, 2009; Jenal et al., 2017; Romling et al., 2013; Ryjenkov et al., 2005; Valentini & Filloux, 2019). The Lyme disease spirochete, *Borrelia burgdorferi* sensu lato, referred to as *Borrelia burgdorferi* henceforth, has a c-di-GMP regulatory network consisting of a transmembrane sensor

This is an open access article under the terms of the [Creative Commons Attribution-NonCommercial](https://creativecommons.org/licenses/by-nc/4.0/) License, which permits use, distribution and reproduction in any medium, provided the original work is properly cited and is not used for commercial purposes.

© 2024 The Authors. *Molecular Microbiology* published by John Wiley & Sons Ltd.

histidine kinase (Hk1), a response regulator diguanylate cyclase (Rrp1), two phosphodiesterases (PdeA and PdeB), and a single, chromosomally encoded PilZ domain-containing protein, PlzA (Caimano et al., 2011; Freedman et al., 2009; Galperin et al., 2001; Novak et al., 2014; Rogers et al., 2009; Sultan et al., 2010, 2011).

The borrelial Hk1/Rrp1 two-component system synthesizes c-di-GMP; activation of Hk1 (BB\_0420) occurs through an unknown signal (Bauer et al., 2015; Caimano et al., 2011). Rrp1 (BB\_0419), the only identified diguanylate cyclase in *B. burgdorferi*, synthesizes c-di-GMP from two GTP molecules and is essential for acquisition and survival in the tick vector (Kostick et al., 2011; Rogers et al., 2009). Turnover of c-di-GMP is mediated by PdeA (BB\_0363) and PdeB (BB\_0374), the only phosphodiesterases present in *B. burgdorferi*, which degrade c-di-GMP to pGpG and GMP, respectively (Sultan et al., 2010, 2011). *B. burgdorferi* must delicately balance c-di-GMP signaling, as c-di-GMP is required for both maintenance in the tick vector and successful transmission into the vertebrate host, but constitutive synthesis is detrimental to spirochete survival during vertebrate infection (Caimano et al., 2015; Groshong et al., 2021; Sultan et al., 2010, 2011).

Synthesized c-di-GMP is bound by PlzA, the only universal c-di-GMP binding protein found in all isolates of Lyme disease *Borrelia* (Kostick-Dunn et al., 2018). Mutation of *plzA* has been implicated in many *B. burgdorferi* phenotypes, including dysregulation of alternative carbohydrate utilization, decreased motility, and virulence defects (Groshong et al., 2021; He et al., 2014; Mallory et al., 2016; Pitzer et al., 2011; Zhang et al., 2018). Binding of c-di-GMP induces conformational changes in PlzA structure, which has led to the hypothesis that c-di-GMP binding acts as a switching mechanism providing the holo and apo-forms of PlzA with distinct functions (Grassmann et al., 2023; Groshong et al., 2021; Mallory et al., 2016). Specifically, c-di-GMP bound PlzA is thought to regulate genes required for survival in the tick host, while apo-PlzA is speculated to play a role in regulation during vertebrate infection (Grassmann et al., 2023; Groshong et al., 2021).

A common mechanism of action for c-di-GMP effector proteins is to bind nucleic acids (Hsieh et al., 2018; Schäper et al., 2017; Skotnicka et al., 2020; Tan et al., 2015; Tschowri et al., 2014; Wang et al., 2016; Wilksch et al., 2011). It has been hypothesized that PlzA could bind DNA and regulate genes through impacts on transcription, such as directly interacting with RNA polymerase (RNAP), but this has yet to be validated experimentally (Grassmann et al., 2023; Groshong et al., 2021). Conversely, others have argued that PlzA cannot bind DNA, as it lacks an obvious, conventional DNA-binding motif (Caimano et al., 2015; Zhang et al., 2018). Indeed, Zhang et al. (2018) concluded that PlzA does not bind DNA, as their electrophoretic mobility shift assays (EMSA) did not identify binding to the *glp* promoter region. We note that the raw data and methodologies, including protein and c-di-GMP concentrations, were not shown in that report. After the submission of a preprint of our manuscript, another group published that PlzA has RNA chaperone activity that is independent of c-di-GMP, supporting the notion that holo- and apo-forms of PlzA have distinct functions (Van Gundy et al., 2023).

Given the multiple conflicting hypotheses regarding PlzA function, as well as the potential for additional mechanisms between liganded and unliganded PlzA, we sought to independently characterize PlzA nucleic acid binding function. To that end, we chose a well-established locus PlzA, which is known to regulate *glpFKD*, the glycerol catabolism operon. The *glpFKD* operon promotes *B. burgdorferi* survival in ticks (Corona & Schwartz, 2015; Helble et al., 2021; Pappas et al., 2011). After a tick has completed the digestion of its blood meal, it is hypothesized that the midgut is devoid of glucose and many other nutrients. To survive in that environment, Lyme disease spirochetes would need to utilize alternate carbon sources such as glycerol, which is available in the tick host (Lee & Baust, 1987). The *glpFKD* operon is regulated through the Hk1/Rrp1 pathway, and borrelial *plzA* mutants are defective in glycerol metabolism (Caimano et al., 2015; He et al., 2011; Rogers et al., 2009; Zhang et al., 2018). Further, PlzA was found to both positively and negatively affect the *glp* operon at higher and lower c-di-GMP levels, respectively (Zhang et al., 2018).

PlzA is classified as an xPilZ-PilZ domain protein, given its dual-domain structure. The binding of c-di-GMP to the interdomain linker and C-terminal PilZ domain results in a conformational change; locking the C-terminal PilZ and N-terminal xPilZ domains into rigid conformation, which we hypothesized could permit DNA binding (Groshong et al., 2021; Mallory et al., 2016; Singh et al., 2021). Although no canonical DNA binding domain is evident in the PlzA amino acid sequence, our lab has discovered and characterized multiple nucleic acid binding proteins possessing novel binding motifs (Babb et al., 2006; Jutras et al., 2012; Jutras, Chenail, Carroll, et al., 2013; Jutras, Chenail, Rowland, et al., 2013; Riley et al., 2009; Singh et al., 2021; Zhang et al., 2018). Here, we report that PlzA can bind DNA and RNA directly downstream of the promoter and into the 5' untranslated region (UTR) of the *glpFKD* operon and that binding to this region is c-di-GMP dependent.

## 2 | RESULTS

### 2.1 | PlzA binds *glpFKD* DNA and the interaction is c-di-GMP dependent

Previous studies demonstrated that c-di-GMP and PlzA modulate expression of the glycerol metabolism operon (Caimano et al., 2015; He et al., 2011; Rogers et al., 2009; Zhang et al., 2018). We hypothesized that PlzA might bind 5' of the *glpFKD* operon. To that end, we sought to determine if PlzA could bind DNA between *glpFKD* and the upstream ORF BB\_0239, which encodes a deoxyguanosine/deoxyadenosine kinase. The transcriptional boundaries and promoter elements of the *glpFKD* operon were previously mapped (Adams et al., 2017; Grove et al., 2017). A fluorescently labeled DNA fragment was generated by PCR amplification from a plasmid containing the 410 bp intergenic region between the upstream gene and the start of *glpF* (BB\_0240) and is denoted as *glpFKD*(-219) (Figure 1).

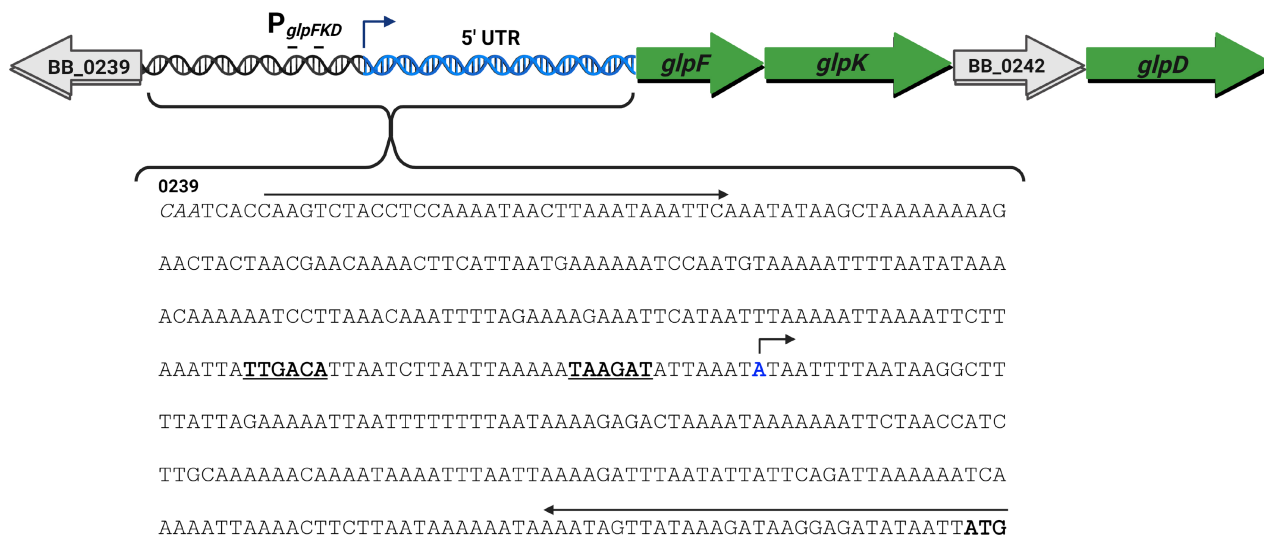


**FIGURE 1** The *glpFKD* operon, 5' UTR, and designed probe schematic. The glycerol catabolism gene operon (*glpFKD*) contains four genes: *glpF* (BB\_0240, glycerol uptake facilitator protein), *glpK* (BB\_0241, glycerol kinase), BB\_0242 (hypothetical protein), and *glpD* (BB\_0243, glycerol-3-phosphate dehydrogenase). The promoter and transcriptional boundaries were previously mapped (Grove et al., 2017). The -35 and -10 sites are bolded and underlined. The transcriptional start site nucleotide is highlighted in blue and topped with an arrow indicating the direction of transcription. The start of the *glpF* ORF is marked by the bolded ATG, whereas the start of the upstream BB\_0239 ORF is labeled, and its nucleotides are italicized. The long arrows indicate the location of primers used to generate a large probe incorporating the entire intergenic region which is denoted as *glpFKD*(-219) for initial DNA binding studies.

To assess if PlzA could bind this DNA, EMSAs with increasing concentrations of recombinant PlzA were performed (Figure 2a). Binding was observed at higher micromolar concentrations, as evidenced by the disappearance of free DNA. The experiment was repeated with added non-specific competitor poly-dI-dC to a final concentration of 2.5 ng/μL. Poly-dI-dC did not appreciably compete away the shifted protein-DNA complexes (Figure 2b).

Given that binding of c-di-GMP has been hypothesized to act as a switching mechanism for PlzA function, we next investigated the effects of c-di-GMP on DNA binding. EMSA reaction mixtures were supplemented with exogenous c-di-GMP to a final concentration of 100 μM. This concentration was used to saturate all PlzA molecules present in the reaction to ensure complete binding throughout electrophoresis. Saturating concentrations have similarly been used in other studies with c-di-GMP binding proteins that also bind DNA (Schäper et al., 2017; Skotnicka et al., 2020; Tan et al., 2015; Wilksch et al., 2011; Yang et al., 2013; Zamorano-Sánchez et al., 2015). The EMSA with *glpFKD*(-219), poly-dI-dC, and increasing PlzA was repeated with the supplemented c-di-GMP (Figure 2c). The addition of c-di-GMP enhanced PlzA binding affinity for *glpFKD*(-219), resulting in binding at lower concentrations of protein, and the formation of distinct protein-DNA complexes as indicated by the arrows. Further, as PlzA concentration increased, the mobility of the shifted band decreased.

To further assess the requirement of c-di-GMP for PlzA DNA binding activity, a mutant PlzA protein (PlzA<sub>RD-RD</sub>) that cannot bind c-di-GMP was produced by site-directed mutagenesis. This mutant replaced key arginine residues in the conserved c-di-GMP binding motif, RxxxR, with aspartic acids (Amikam & Galperin, 2006; Chou & Galperin, 2016; Ryjenkov et al., 2006). These mutations (R145D and

R149D) have previously been shown to abolish c-di-GMP binding (Freedman et al., 2009; Mallory et al., 2016; Singh et al., 2021). The *glpFKD*(-219) EMSAs were repeated with PlzA<sub>RD-RD</sub> (Figure 2d-f). Binding to *glpFKD*(-219) was not observed under any tested conditions with PlzA<sub>RD-RD</sub>.

To ensure binding was not due to the recognition of vector-derived sequences within the probe, competition EMSAs were performed with unlabeled DNA competitors derived from empty pCR 2.1 TA clones, or those containing the *glpFKD*(-219) sequence (Figure S1). The nonspecific DNA from the empty pCR 2.1 vector did not compete away PlzA<sub>WT</sub>-*glpFKD*(-219) complexes at a 20-fold higher concentration (Figure S1b, lanes 3–5). Meanwhile, as little as 6-fold molar excess of unlabeled *glpFKD*(-219) was able to compete with the probe, and a 10-fold molar excess successfully competed away the PlzA<sub>WT</sub>-*glpFKD*(-219) complexes (Figure S1b, lanes 6–8). These results demonstrate that PlzA preferentially bound the *glpFKD*-derived sequences.

Noting that c-di-GMP enhanced DNA binding by PlzA, yet free DNA decreased with purified recombinant PlzA without adding exogenous c-di-GMP, we investigated the possibility that PlzA was being purified with c-di-GMP already bound. Purified recombinant proteins were prepared and assayed by liquid chromatography-tandem mass spectrometry. Extracted ion chromatograms showed the presence of c-di-GMP in PlzA<sub>WT</sub> protein preparations but not in PlzA<sub>RD-RD</sub> preparations (Figure 3). The concentration of c-di-GMP present in recombinant PlzA<sub>WT</sub> was extrapolated from a c-di-GMP standard curve at 99.29 nM. A total of 31.7 μM of protein had been analyzed, indicating that approximately 0.3% of the protein was bound with c-di-GMP. Prior studies have reported dissociation constants of 1.25 to 6.25 μM of PlzA for c-di-GMP, which are typical

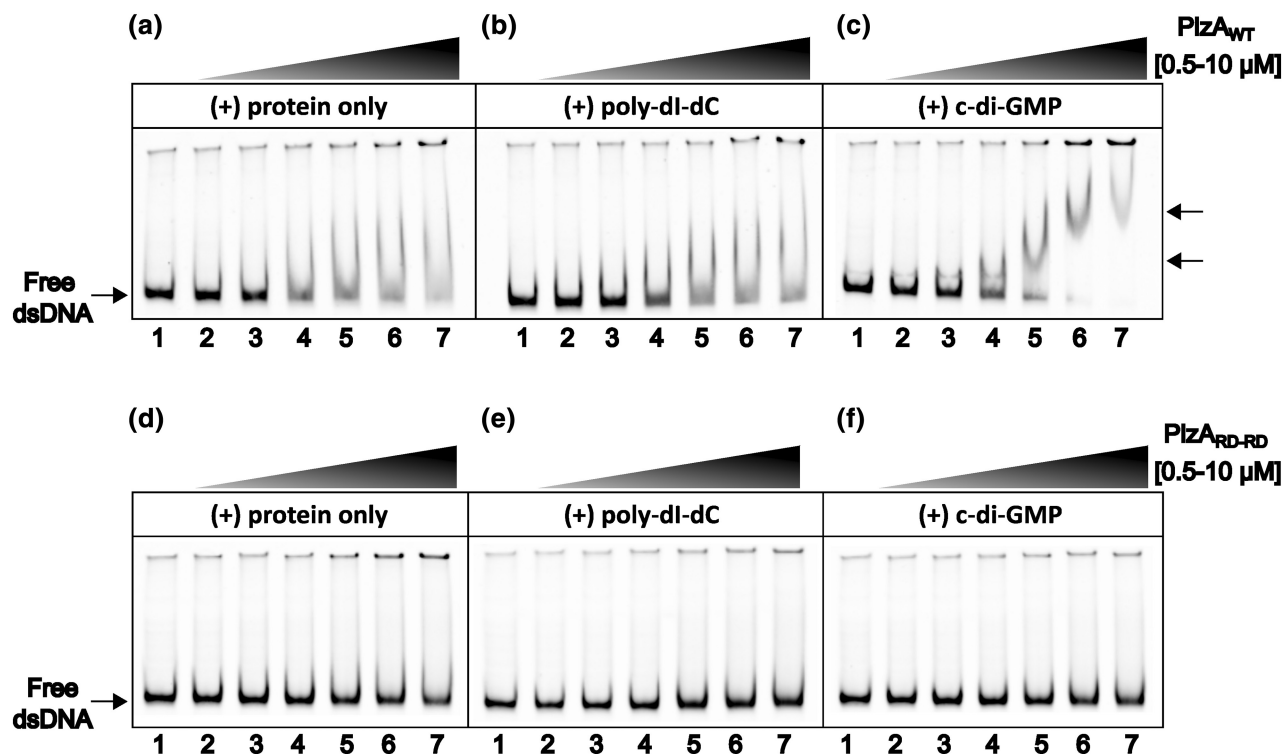


**FIGURE 2** DNA binding by PlzA is c-di-GMP dependent. (a) EMSA with increasing concentrations of PlzA<sub>WT</sub> showing binding to *glpFKD*(-219) DNA. The mixture was incubated for 10 min before electrophoresis. (b) The same EMSA mixture as in (a) but with a final concentration of 2.5 ng/μL of the nonspecific competitor poly-dI-dC. Protein was incubated with poly-dI-dC for 5 min prior to the addition of labeled *glpFKD*(-219) probe. (c) The same EMSA mixture as in (b) but supplemented with 100 μM c-di-GMP. Protein was incubated with c-di-GMP for 5 min prior to the addition of any nucleic acids. Arrows indicate PlzA-*glpFKD*(-219) complexes. Lane 1 in (a-c) is the probe only control, containing 50 nM of probe. Protein concentrations are as follows in each subsequent lane: Lane 2: 0.5 μM, Lane 3: 1 μM, Lane 4: 2.5 μM, Lane 5: 5 μM, Lane 6: 7.5 μM, and Lane 7: 10 μM. (d-f) EMSA experiments as in (a-c), respectively, but performed with the mutant PlzA<sub>RD-RD</sub> protein. All conditions were performed identically as with PlzA<sub>WT</sub>. Each panel is a representative gel from separate EMSAs which were performed in triplicate (PlzA<sub>WT</sub>) or duplicate (PlzA<sub>RD-RD</sub>).

### c-di-GMP; [M-H]<sup>-</sup> = m/z 689.09

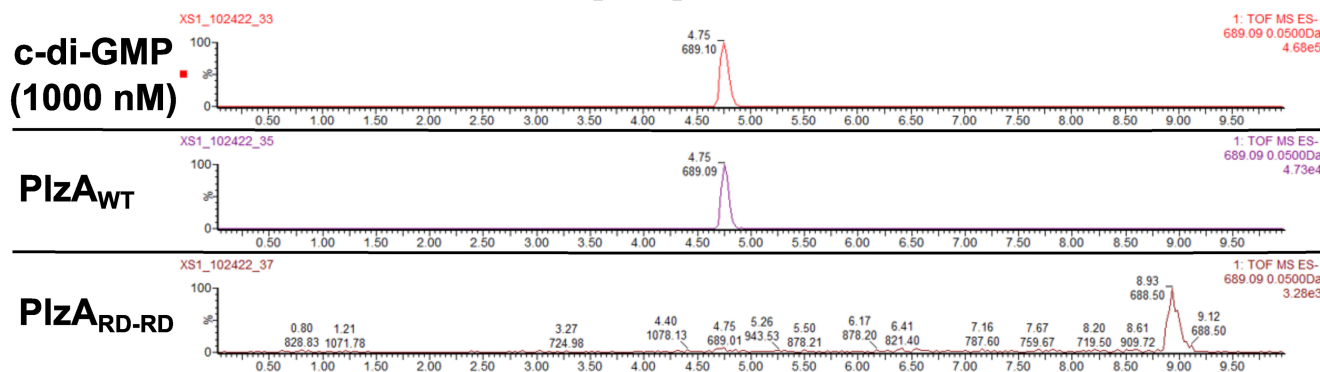


**FIGURE 3** Detection of c-di-GMP in recombinant PlzA<sub>WT</sub> and PlzA<sub>RD-RD</sub> by LC-MS/MS. Recombinant PlzA<sub>WT</sub> and PlzA<sub>RD-RD</sub> were sent off for mass spectrometry to detect c-di-GMP. Extracted ion chromatograms of the LC-MS/MS analysis for detection of c-di-GMP are displayed. Chromatograms depict the control c-di-GMP standard at 1 μM, recombinant PlzA<sub>WT</sub>, and recombinant PlzA<sub>RD-RD</sub>. The LC-MS/MS analysis reveals PlzA<sub>WT</sub> co-purified with c-di-GMP, but PlzA<sub>RD-RD</sub> did not. The concentration of c-di-GMP in recombinant PlzA<sub>WT</sub> was determined from a standard curve of c-di-GMP. PlzA<sub>WT</sub> co-purified with 99.29 nM of c-di-GMP and approximately 0.3% of the protein was bound with c-di-GMP. Black lines indicate chromatograms unrelated to this figure that were removed.

$K_D$  values for PilZ receptors and c-di-GMP (Mallory et al., 2016; Pitzer et al., 2011). The amount of co-purified c-di-GMP detected is lower than the  $K_D$ . This is likely due to removal of some c-di-GMP

during the protein purification process, as well as *Escherichia coli* maintaining low cellular concentrations of c-di-GMP (~40–80 nM) (Junkermeier & Hengge, 2023; Sarenko et al., 2017). Taken together,

these data indicate that PlzA DNA binding to this region of the *glpFKD* operon is specific and c-di-GMP dependent.

## 2.2 | c-di-GMP levels modulate PlzA DNA binding affinity

It was previously identified with *glpFKD-gfp* promoter fusion studies that the minimal *glpFKD* promoter sequence (−46 relative to the *glpFKD* transcription start site) with the full 195 bp UTR region was expressed at higher levels than the core promoter sequence alone (Grove et al., 2017). Given these findings and our data that PlzA can bind DNA, we focused further analysis of PlzA binding on a smaller sequence within that region that was found to be important for regulation (Grove et al., 2017; Savage et al., 2018). A 42 bp DNA probe encompassing the −7 to +35 sites, called *glpFKD*(−7/+35), was generated by annealing complementary oligonucleotides with the forward oligonucleotide 5′ conjugated to IRDye800 (Figure 4a). An RNA probe conjugated to Alexa Fluor 488 was also made for subsequent RNA binding studies.

To determine how different c-di-GMP levels impact PlzA binding affinity, EMSAs with increasing PlzA<sub>WT</sub> concentrations were performed at concentrations of added c-di-GMP ranging from 0 to 100 μM in the reaction mixtures with the *glpFKD*(−7/+35) probe (Figure 4b). Competitor poly-dI-dC was added at a final concentration of 2.5 ng/μL to reduce nonspecific interactions. PlzA<sub>WT</sub> bound to *glpFKD*(−7/+35) and binding was enhanced by increasing the concentration of c-di-GMP. In reactions with no added c-di-GMP, we observed that the amount of free DNA decreased with increasing PlzA concentrations but did not detect a band corresponding to the protein-DNA complex. The decrease in free DNA with no added c-di-GMP is presumably due to the presence of co-purified c-di-GMP in recombinant PlzA. When equimolar c-di-GMP and protein levels were tested, a discernable shift (formation of a new band) was evident only at protein concentrations greater than 2.5 μM (purple arrow). As c-di-GMP concentrations were further increased, shifts became discernable at lower protein concentrations, with the strongest binding observed at c-di-GMP concentrations of 25, 50, and 100 μM. Further, as protein concentration was increased, we consistently observed progressive super-shifting of complexes in a dose-dependent manner (Figure 4b, colored arrows). At protein concentrations greater than or equal to 5 μM coupled with c-di-GMP concentrations greater than 25 μM, complexes appeared to smear, suggesting the observed super-shifting is due to complex dissociation. The stoichiometry of this complex(es) is under investigation.

Next, we calculated the apparent binding affinity ( $K_{D(\text{app})}$ ) under these experimental conditions for PlzA for *glpFKD*(−7/+35) at the various c-di-GMP concentrations (Figure 4c). The calculations were performed under the assumption that a single molecule of PlzA binds to a single molecule of DNA. As noted above, it is possible that the protein-nucleic acid ratio is not 1:1, which could affect the calculated values. The values described below are the  $K_{D(\text{app})} \pm \text{SEM}$  (standard error of the mean). Without any supplemented c-di-GMP,

the extrapolated  $K_{D(\text{app})}$  of PlzA<sub>WT</sub>-*glpFKD*(−7/+35) was calculated as 7.86 ( $\pm 1.84 \mu\text{M}$ ). However, we again note that some c-di-GMP is already present in the PlzA<sub>WT</sub> protein preparations (see above and Figure 3). Binding affinity increased approximately 1.5-fold under equimolar c-di-GMP and protein concentrations with a calculated  $K_{D(\text{app})}$  of 4.22 ( $\pm 0.43 \mu\text{M}$ ). Under saturating c-di-GMP conditions (exceeding the  $K_D$  of PlzA for c-di-GMP), binding affinity increased further. Supplementing binding reactions with 10 μM c-di-GMP improved PlzA-DNA binding 2.5-fold with a  $K_{D(\text{app})}$  of 2.81 ( $\pm 0.50 \mu\text{M}$ ). An approximately 6- to 7-fold increase in binding affinity was observed when the binding reaction was supplemented with either 25, 50, or 100 μM of c-di-GMP resulting in calculated  $K_{D(\text{app})}$ s of 1.33 ( $\pm 0.12 \mu\text{M}$ ), 1.25 ( $\pm 0.08 \mu\text{M}$ ), and 1.09 μM ( $\pm 0.06 \mu\text{M}$ ), respectively.

To determine if the calculated  $K_{D(\text{app})}$  values differed significantly, Welch's ANOVA followed by a Dunnett's T3 multiple comparisons test was performed (Figure 4d). All calculated  $K_{D(\text{app})}$  values differed significantly ( $p < 0.05$ ) from the 0 μM c-di-GMP  $K_{D(\text{app})}$  except for the equimolar and 10 μM c-di-GMP conditions. Compared to the equimolar condition, the 25, 50, and 100 μM  $K_{D(\text{app})}$  values differed significantly ( $p < 0.001$ ), while the 10 μM c-di-GMP  $K_{D(\text{app})}$  value did not ( $p > 0.05$ ). When comparing the 10, 25, 50, and 100 μM  $K_{D(\text{app})}$  values of PlzA<sub>WT</sub>-*glpFKD*(−7/+35) interaction, there were no significant differences ( $p > 0.05$ ). The mutant PlzA<sub>RD-RD</sub> did not bind *glpFKD*(−7/+35) under any tested conditions (Figure 4e). Overall, we conclude that levels of c-di-GMP significantly impact PlzA-DNA binding.

## 2.3 | PlzA interacts predominantly with the major groove of DNA and sequence length appears to play a role in DNA binding affinity

We next sought to gain further information on the mode of binding between PlzA and dsDNA. To explore these interactions, we performed binding assays with methyl green and actinomycin D which bind the major and minor grooves of DNA, respectively (Basu et al., 2009; Kim & Nordén, 1993; Liu et al., 2016; Shi et al., 2022). EMSAs were performed with increasing concentrations of these drugs to determine if either could compete with PlzA<sub>WT</sub> for binding to the *glpFKD*(−7/+35) probe (Figure 5). Methyl green was able to compete for binding as evidenced by the increase in free DNA and by the disruption of PlzA-*glpFKD*(−7/+35) complex formation at higher concentrations. Oppositely, competition with actinomycin D was only evident at the highest concentrations tested. These results indicate that PlzA interacts with dsDNA mainly through interactions with the major groove.

To gain insights into the DNA sequence requirements for PlzA binding, the *glpFKD*(−7/+35) sequence was changed at several nucleotides (Figure 6a). Mutant competitors 1 and 2 targeted the middle region of the sequence containing one of the few GC rich regions. To introduce greater G-C content and potentially disrupt symmetry, mutant competitors 3–5 swapped an ATTA repeat to CGGC at the 5′, 3′ or both ends. In the mutant competitor 6 sequence, a middle

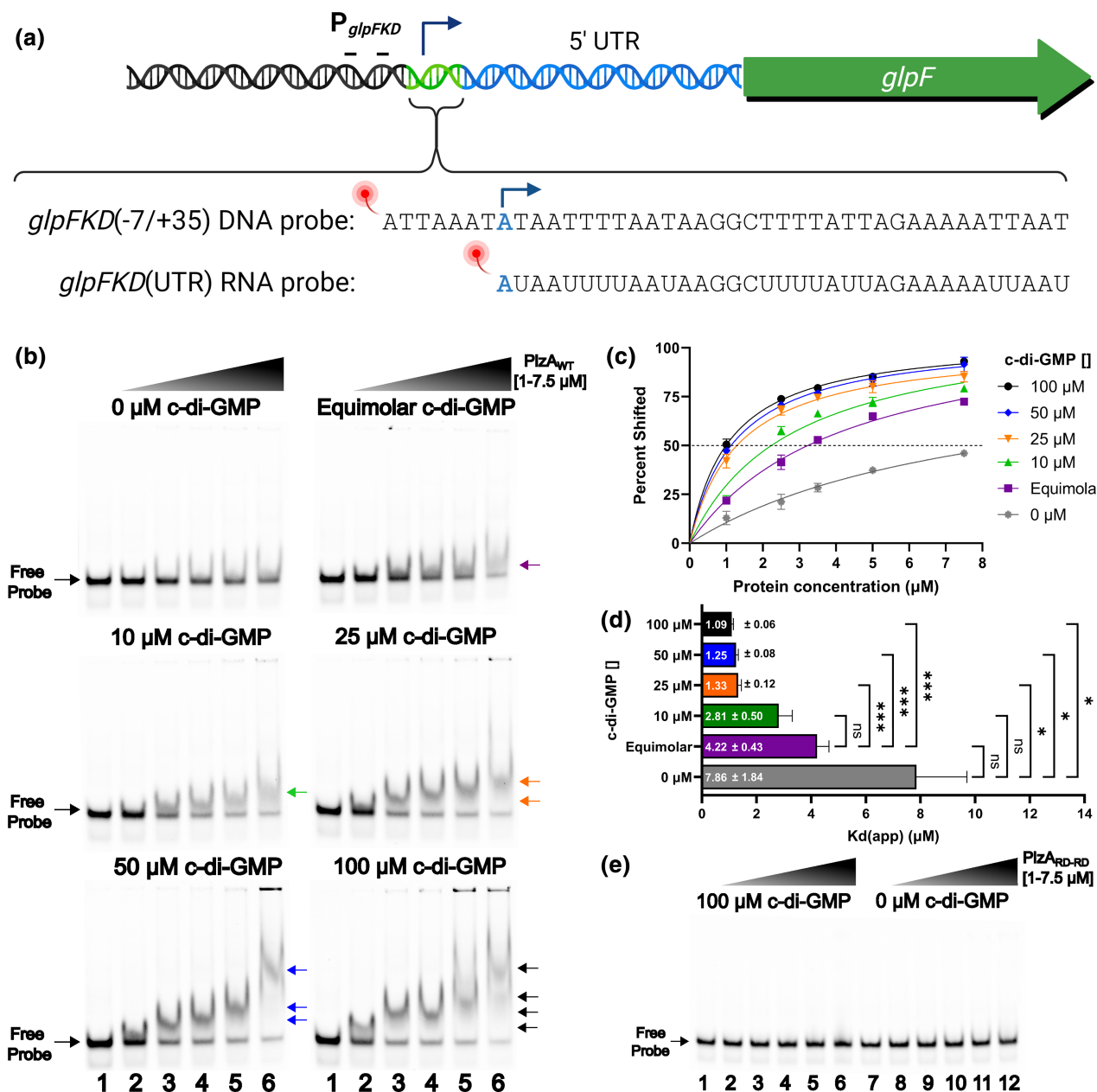


**FIGURE 4** Levels of c-di-GMP alter DNA binding affinity of PlzA<sub>WT</sub>. (a) A diagram of the generated DNA probe, designated as *glpFKD*(-7/+35), corresponding to a 42bp sequence adjacent to the -10 site and proceeding 35bp into the 5' UTR. An RNA probe was made corresponding to only nucleotides that are within the 5'UTR which was designated as *glpFKD*(UTR) RNA. Probes were conjugated to a fluorescent molecule for the detection of binding in EMSAs. (b) EMSAs were performed with increasing protein concentrations of PlzA<sub>WT</sub>, and 10nM fluorescently labeled probe at varying c-di-GMP concentrations (0, equimolar, 10, 25, 50, or 100  $\mu\text{M}$ ). For each EMSA shown, the indicated c-di-GMP concentration was held constant in all lanes. For each EMSA shown, lanes 1 and 7 are probe-only controls. Protein concentrations were as follows: Lane 2: 1  $\mu\text{M}$ , Lane 3: 2.5  $\mu\text{M}$ , Lane 4: 3.5  $\mu\text{M}$ , Lane 5: 5  $\mu\text{M}$ , Lane 6: 7.5  $\mu\text{M}$ . A final concentration of 2.5 ng/ $\mu\text{L}$  of the nonspecific competitor poly-dI-dC was added to each lane. Arrows indicate higher-order complexes formed as protein concentration increases. A representative gel for each tested c-di-GMP concentration is shown from triplicate EMSAs. (c) Triplicate EMSAs were quantitated by densitometry to determine the  $K_{d(app)}$  of the PlzA<sub>WT</sub>-*glpFKD*(-7/35+) interaction by nonlinear regression analysis using the one-site specific binding setting in GraphPad Prism. Errors bars represent one standard deviation (SD). (d) Bar graph displaying the calculated  $K_{d(app)} \pm$  the standard error of the mean (SEM). The  $K_{d(app)}$  values from three EMSAs were analyzed by a Welch ANOVA with Dunnett's T3 multiple comparisons test via GraphPad Prism. Adjusted  $p$ -values are indicated as follows: <sup>ns</sup> $p > 0.05$ , \* $p < 0.05$ , and \*\*\* $p < 0.001$ . Comparisons between 10, 25, 50, and 100  $\mu\text{M}$  c-di-GMP are not indicated on the graph as they were not significant. (e) A similar EMSA experiment was performed as in Figure 4b but with PlzA<sub>RD-RD</sub> and either 100 (lanes 1-6) or 0 (lanes 7-12)  $\mu\text{M}$  of c-di-GMP supplemented. No binding is observed.

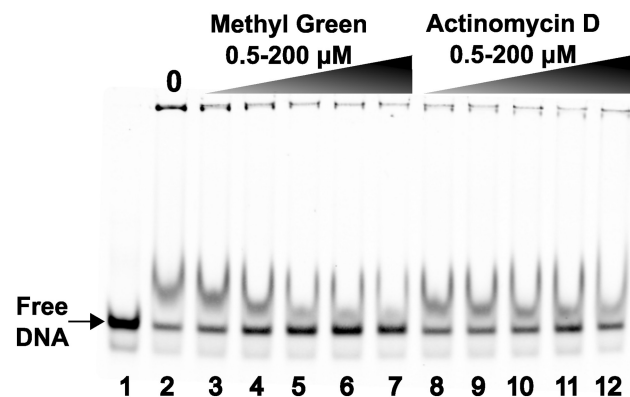


**FIGURE 5** Major and Minor Groove Binding Assay. Competition EMSAs were performed with a constant PlzA<sub>WT</sub> concentration of 3.5  $\mu$ M, 10 nM fluorescently labeled *glpFKD(-7/+35)* probe, and a constant c-di-GMP concentration of 100  $\mu$ M. Lane 1 is the probe-only control, while lane 2 is the probe + protein only control. Lanes 3–7 contain increasing concentrations of methyl green: Lane 3: 0.5  $\mu$ M, Lane 4: 5  $\mu$ M, Lane 5: 50  $\mu$ M, Lane 6: 3100  $\mu$ M, and Lane 7: 200  $\mu$ M. Lanes 8–12 contain increasing concentrations of Actinomycin D: Lane 8: 0.5  $\mu$ M, Lane 9: 5  $\mu$ M, Lane 10: 50  $\mu$ M, Lane 11: 100  $\mu$ M and Lane 12: 200  $\mu$ M. A representative gel is shown from three independently performed experiments.

section with a run of Ts, TTTTAA, is changed to GGGGCC. Lastly, competitors 7–9 were designed to disrupt potential secondary structural elements. Competition EMSAs with the IRDye labeled *glpFKD(-7/+35)* probe, the unlabeled *glpFKD(-7/+35)* specific competitor, and the unlabeled mutagenized competitors were performed with PlzA<sub>WT</sub> (Figure 6b).

Despite introducing various mutations into the *glpFKD(-7/+35)* sequence, competition still occurred, although some sequences competed better than others. Mutant competitors 1 and 2 competed similarly to the unlabeled specific competitor indicating the mutations did not disrupt PlzA recognition and binding. An increase in the sequence G–C content (mutant competitors 3–9) resulted in some decreased competition, suggesting PlzA could have higher affinity for A–T rich sequences. Overall, our results suggest that the *glpFKD(-7/+35)* sequence may be a non-consensus or low-affinity DNA binding site of PlzA within the *glpFKD* operon. This 42bp sequence was chosen as it is crucial for *glpFKD* regulation and is known to be bound by other proteins (Grove et al., 2017; Savage et al., 2018; Saylor et al., 2023; Zhang et al., 2024). We hypothesize that there could be higher affinity binding sites upstream of this operon and within the *B. burgdorferi* genome.

Since we could not identify an obvious PlzA sequence motif, we next investigated if PlzA bound DNA in a length-dependent mechanism. The *glpFKD(-7/+35)* sequence was truncated by nine bases at the 5' end and then an additional three nucleotides at a time, and competition EMSAs were performed with these DNAs (Figure 7). The truncated *glpFKD(-7/+35)* competitors exhibited less competition than the unlabeled specific competitor (Comp 1/C1) at the same concentration (Figure 7b). This could indicate that the nucleotides removed from the 5' end are necessary for PlzA recognition or that PlzA

has a higher affinity for longer pieces of DNA. Studies are ongoing to determine how PlzA recognizes nucleic acids and to find additional PlzA binding sites, as further elaborated upon in the discussion.

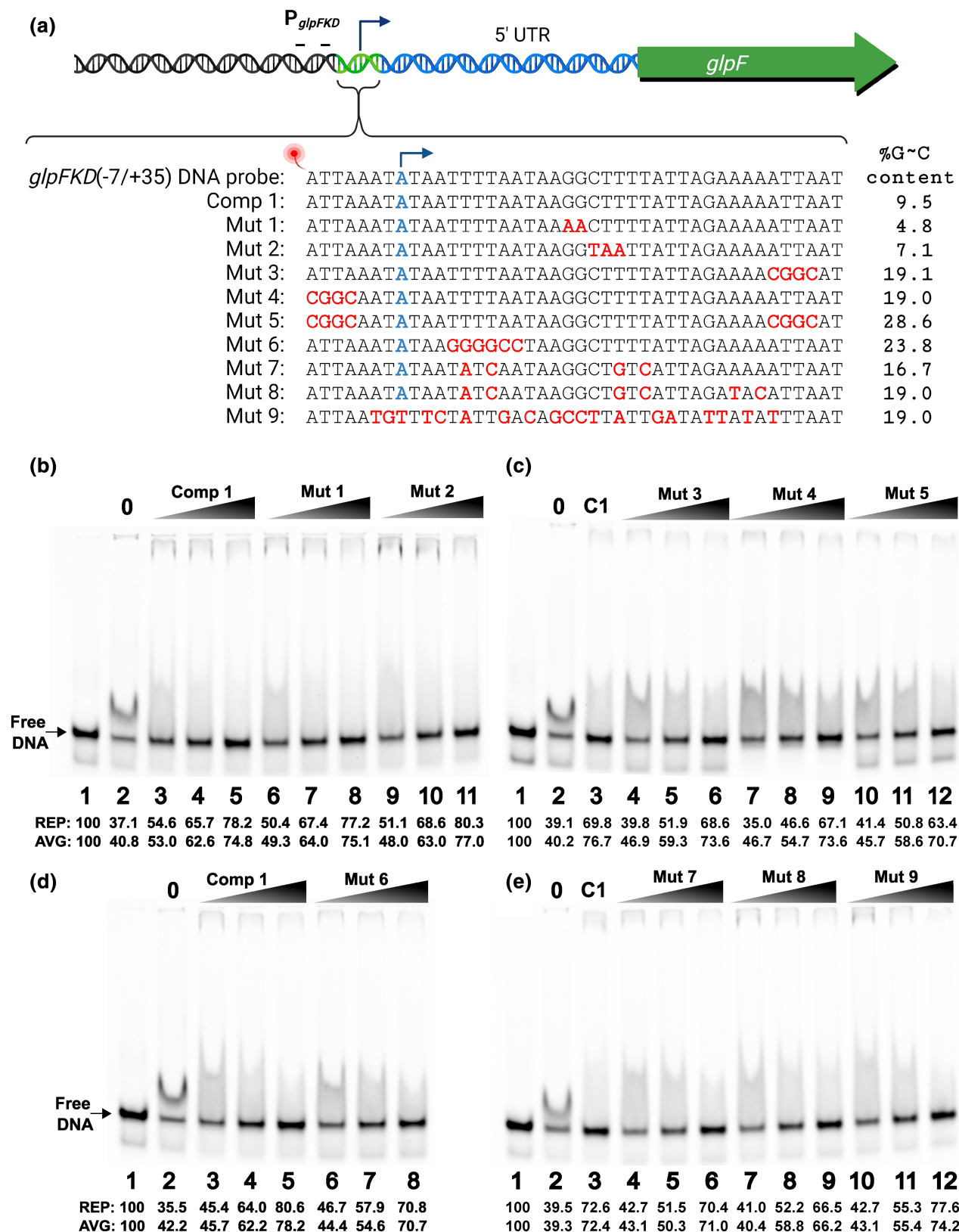
## 2.4 | PlzA also binds *glp*-derived single-stranded nucleic acids

Several borrelial proteins that were initially identified as having affinities for DNA have subsequently been found to also bind RNA (Jutras, Chenail, Carroll, et al., 2013; Krusenstjerna et al., 2023; Savage et al., 2018). Given the role the 5' UTR of the *glpFKD* operon plays in its regulation, we hypothesized PlzA could potentially also bind RNA. RNA probes used were designed to correspond to only transcribed regions (Figure 4a). The *glpFKD(-7/+35)* counterpart RNA probe is designated *glpFKD(UTR)*. EMSAs were performed with increasing concentrations of PlzA<sub>WT</sub> with 0  $\mu$ M, 100  $\mu$ M, or equimolar c-di-GMP levels and labeled *glpFKD(UTR)* (Figure 8). PlzA<sub>WT</sub> bound the RNA, which was enhanced by addition of c-di-GMP (Figure 8a). The binding pattern to the *glpFKD(UTR)* RNA was comparable to the *glpFKD(-7/+35)* DNA, with increased protein and c-di-GMP concentrations leading to an increased size of the PlzA-RNA shifts.

EMSAs were repeated with the PlzA<sub>RD-RD</sub> mutant protein at 0 or 100  $\mu$ M c-di-GMP (Figure 8b). The PlzA<sub>RD-RD</sub> protein did not bind *glpFKD(UTR)* RNA at any tested protein concentration, regardless of whether c-di-GMP was included.

Given that PlzA can bind to both the DNA and RNA, we sought to determine if it could also bind the cognate ssDNA corresponding to the coding strand. This is relevant as ssDNA is exposed at open transcriptional complexes. The forward, IRDye labeled oligonucleotide used to generate the *glpFKD(-7/+35)* dsDNA probe was used as a single-stranded DNA probe (*ssglpF*) in EMSAs. No evident complexes were formed when exogenous c-di-GMP was excluded from EMSA reactions, but free ssDNA did decrease at the highest tested PlzA concentrations of 3.5–7.5  $\mu$ M (Figure 8c right panel). Adding 100  $\mu$ M c-di-GMP resulted in the formation of PlzA-ssDNA complexes but at higher concentrations of protein than required to achieve complex formation with dsDNA and RNA (Figure 8c left panel).

We next quantified the binding affinity of PlzA for the *glp*-derived RNA and ssDNA sequences through densitometry of the EMSA shifts, and the apparent  $K_{D(app)}$ s calculated as described above (Figure 4d). As with dsDNA, the binding affinity of PlzA for RNA was weakest when no exogenous c-di-GMP was supplemented with a calculated  $K_{D(app)}$  of 7.64 ( $\pm$  1.85  $\mu$ M). Binding improved approximately 2-fold in equimolar c-di-GMP conditions with a  $K_{D(app)}$  of 4.14 ( $\pm$  0.74  $\mu$ M). The  $K_{D(app)}$  was 0.95 ( $\pm$  0.11  $\mu$ M) when the c-di-GMP concentration was 100  $\mu$ M, an 8-fold increase in PlzA binding affinity for the *glpFKD(UTR)* RNA as compared to when no c-di-GMP was added. There was a significant difference between the PlzA<sub>WT</sub>-*glpFKD(UTR)* RNA  $K_{D(app)}$  value calculated at 100  $\mu$ M c-di-GMP and both the equimolar and 0  $\mu$ M c-di-GMP values ( $p$  < 0.01) (Figure 9a). No significant differences were detected between the  $K_{D(app)}$  values calculated at 0  $\mu$ M and equimolar c-di-GMP levels ( $p$  > 0.05).



Although PlzA bound the *ssglpF* probe, it had a substantially lower affinity for ssDNA than dsDNA or RNA (Figure 8d). The  $K_{D(\text{app})}$  of the PlzA<sub>WT</sub>-*ssglpF* interaction was 8.74 ( $\pm 1.86$   $\mu\text{M}$ ) with 0  $\mu\text{M}$  c-di-GMP and 4.42 ( $\pm 0.90$   $\mu\text{M}$ ) with 100  $\mu\text{M}$  c-di-GMP. These values were found to be statistically significant from one another

( $p < 0.05$ ) (Figure 9b). Only a 2-fold increase in binding affinity of PlzA for the single-strand DNA was observed when the c-di-GMP concentration was increased to 100  $\mu\text{M}$ , whereas the same concentration of c-di-GMP increased PlzA binding affinity 7-fold for dsDNA and 8-fold for RNA.

**FIGURE 6** Competition EMSAs with mutagenized *glpFKD(-7/35+)* competitors. (a) A diagram of the generated unlabeled, mutagenized *glpFKD(-7/+35)* competitors. Comp 1 (C1) is the unlabeled, specific *glpFKD(-7/+35)* competitor. Introduced mutations are indicated in red for each mutant competitor. The transcriptional start site is the nucleotide labeled as blue. Competition EMSAs were performed with the various mutant competitors and the *glpFKD(-7/35+)* probe. For these competitions, the final concentrations of  $PlzA_{WT}$ , c-di-GMP, poly-dl-dC, and *glpFKD(-7/35+)* probe were held constant at 2.5  $\mu$ M, 100  $\mu$ M, 2.5 ng/ $\mu$ L, and 10 nM respectively in all panels shown. (b) Lane 1 is the probe-only control, while lane 2 is the probe + protein only control. Lanes 3–5: 250, 500, & 1000x molar excess (relative to the probe) of specific comp 1. Lanes 6–8: 250, 500, & 1000x mut 1 competitor. Lanes 9–11: 250, 500, & 1000x mut 2 competitor. (c) Lane 1 is the probe-only control, while lane 2 is the probe + protein only control. Lane 3 is the specific competitor control with 1000x of comp 1. Lanes 4–6: 250, 500, & 1000x mut 3 competitor. Lanes 7–9: 250, 500, & 1000x mut 4 competitor. Lanes 10–12: 250, 500, & 1000x mut 5 competitor. (d) Lane 1 is the probe-only control, while lane 2 is the probe + protein only control. Lanes 3–5: 250, 500, & 1000x molar excess of specific comp 1. Lanes 6–8: 250, 500, & 1000x mut 6 competitor. (e) Lane 1 is the probe-only control, while lane 2 is the probe + protein only control. Lane 3 is the specific competitor control with 1000x of comp 1. Lanes 4–6: 250, 500, & 1000x mut 7 competitor. Lanes 7–9: 250, 500, & 1000x mut 8 competitor. Lanes 10–12: 250, 500, & 1000x mut 9 competitor. A representative gel is shown in each panel from an EMSA performed in duplicate. The normalized band percentage values of the free probe are shown below the lane designations in each panel for the representative gel (REP) as well as for the average (AVG) of the duplicate EMSAs.

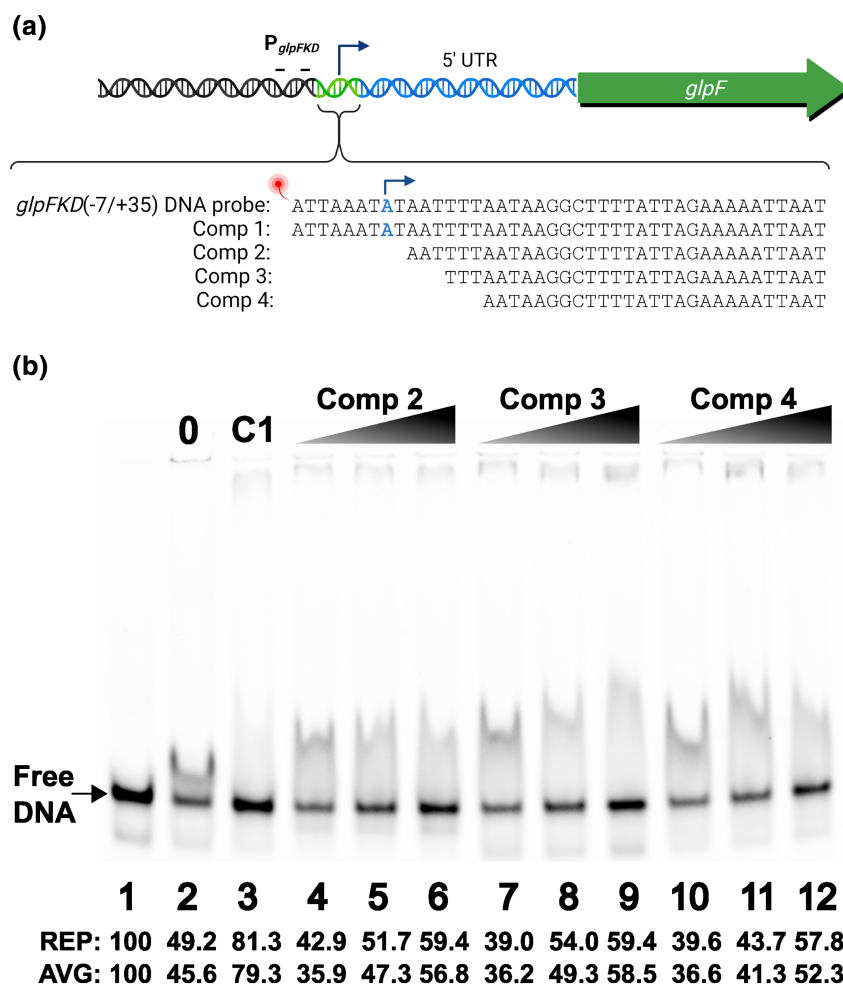


**FIGURE 7** Competition EMSAs with truncated *glpFKD(-7/35+)* competitors. (a) A diagram of the generated unlabeled, truncated *glpFKD(-7/+35)* competitors. Comp 1 (C1) is the unlabeled, specific *glpFKD(-7/+35)* competitor. Competitors 2, 3, and 4 are unlabeled *glpFKD(-7/+35)* truncated at the 5' end by either 9, 12, or 15 bases respectively. The transcriptional start site is the nucleotide labeled as blue. (b)  $PlzA_{WT}$ , c-di-GMP, poly-dl-dC, and *glpFKD(-7/35+)* probe concentrations were held constant at 2.0  $\mu$ M, 100  $\mu$ M, 2.5 ng/ $\mu$ L, and 10 nM respectively. Lane 1 is the probe-only control, while lane 2 is the probe + protein only control. Lane 3 is the specific competitor control with 1000x of comp 1. Lanes 4–6: 250, 500, & 1000x comp 2 competitor. Lanes 7–9: 250, 500, & 1000x comp 3 competitor. Lanes 10–12: 250, 500, & 1000x comp 4 competitor. A representative gel is shown from three independently performed experiments. The normalized band percentage values of the free probe are shown below the lane designations in each panel for the representative gel (REP) as well as for the average (AVG) values from the triplicate EMSAs. The C1 AVG value was calculated from two experiments only.

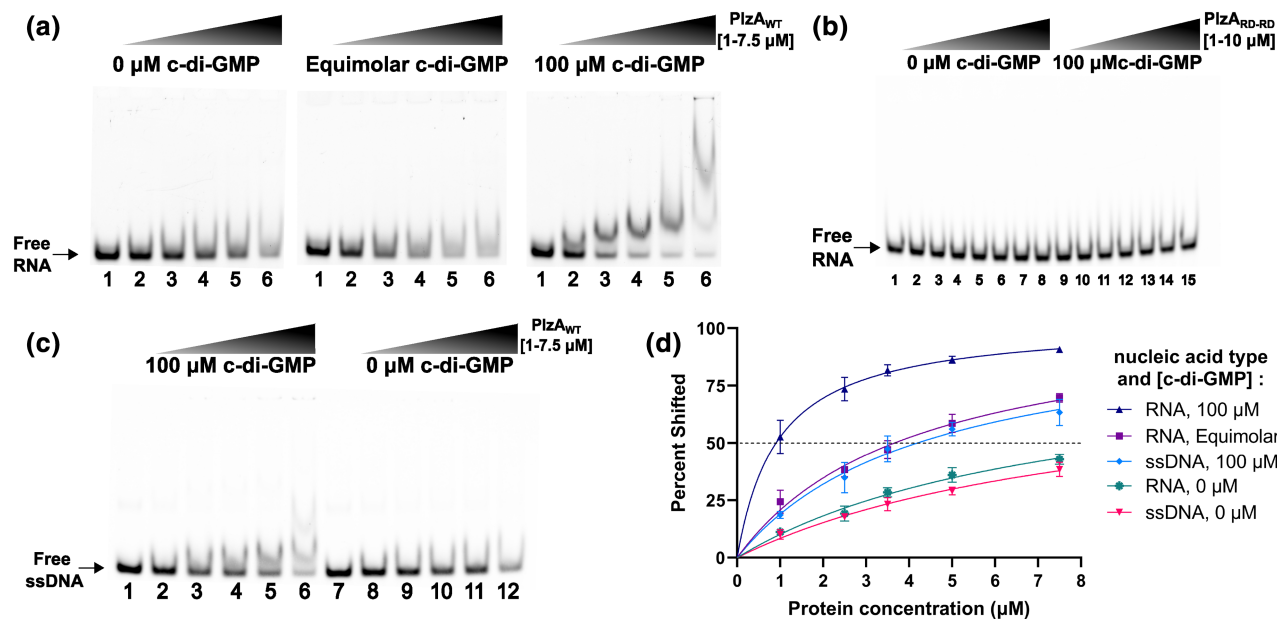


**FIGURE 8** PlzA<sub>WT</sub> also binds single stranded RNA and DNA. (a) Gradient EMSAs were performed with increasing protein concentrations of PlzA<sub>WT</sub> without c-di-GMP (left panel), equimolar (middle panel), or 100 μM c-di-GMP (right panel) and 10 nM fluorescently labeled *glpFKD*(UTR) RNA probe. Lane 1 is the probe-only control in each EMSA. Lane protein concentrations were as follows: Lane 2: 1 μM, Lane 3: 2.5 μM, Lane 4: 3.5 μM, Lane 5: 5 μM, Lane 6: 7.5 μM. (b) A similar EMSA experiment was performed with PlzA<sub>RD-RD</sub> with (lanes 1–8) or without (lanes 9–15) 100 μM c-di-GMP and 50 nM of *glpFKD*(UTR) RNA probe. Lane 1 is a probe-only control. Protein concentrations were as follows: Lanes 2 and 9: 1 μM, Lanes 3 and 10: 1.25 μM, Lanes 4 and 11: 2 μM, Lanes 5 and 12: 2.5 μM, Lanes 6 and 13: 3.3 μM, Lanes 7 and 14: 5 μM, Lanes 8 and 15: 10 μM. Riboguard was supplemented in the PlzA<sub>RD-RD</sub> EMSA mixtures to a final concentration of 4 U/μL. (c) Gradient EMSAs were performed with increasing protein concentrations of PlzA<sub>WT</sub> with 100 μM c-di-GMP (left panel) or 0 μM c-di-GMP (right panel) with 10 nM fluorescently labeled *ssgfp* probe. Lanes 1 and 7 are the probe-only control in each EMSA. Lane protein concentrations were as follows: Lanes 2 and 8: 1 μM, Lanes 3 and 9: 2.5 μM, Lanes 4 and 10: 3.5 μM, Lanes 5 and 11: 5 μM, Lanes 6 and 12: 7.5 μM. Representative gels are shown from triplicate (PlzA<sub>WT</sub>) or duplicate (PlzA<sub>RD-RD</sub>) EMSA experiments. (d) Triplicate EMSAs from (a) and (c) were quantitated by densitometry to determine the  $K_{d(\text{app})}$  of PlzA<sub>WT</sub> for the *glpFKD* RNA or ssDNA interactions by nonlinear regression analysis using the one-site specific binding setting in GraphPad Prism. Errors bars represent one standard deviation (SD).

Lastly, we also compared the binding affinities of PlzA for all three tested nucleic acids (Figure 9c). The calculated  $K_{d(\text{app})}$  values of PlzA<sub>WT</sub> for each nucleic acid in the presence of 100 μM c-di-GMP were compared with a Welch's ANOVA and Dunnett's T3 multiple comparisons test. No significant difference ( $p > 0.05$ ) was detected between the PlzA  $K_{d(\text{app})}$  values for dsDNA ( $1.09 \pm 0.06 \mu\text{M}$ ) and RNA ( $0.95 \pm 0.11 \mu\text{M}$ ), indicating that PlzA binds the *glpFKD* dsDNA and RNA with similar affinity. Both the dsDNA and RNA  $K_{d(\text{app})}$ s were significantly different from the calculated ssDNA  $K_{d(\text{app})}$  ( $4.42 \pm 0.90 \mu\text{M}$ ) ( $p < 0.01$ ), suggesting that PlzA prefers *glp*-derived dsDNA and RNA over ssDNA. All the binding data presented throughout the manuscript are summarized in Table 1. Collectively, our data indicate that PlzA binding activity is c-di-GMP dependent for all tested *glpFKD* nucleic acids.

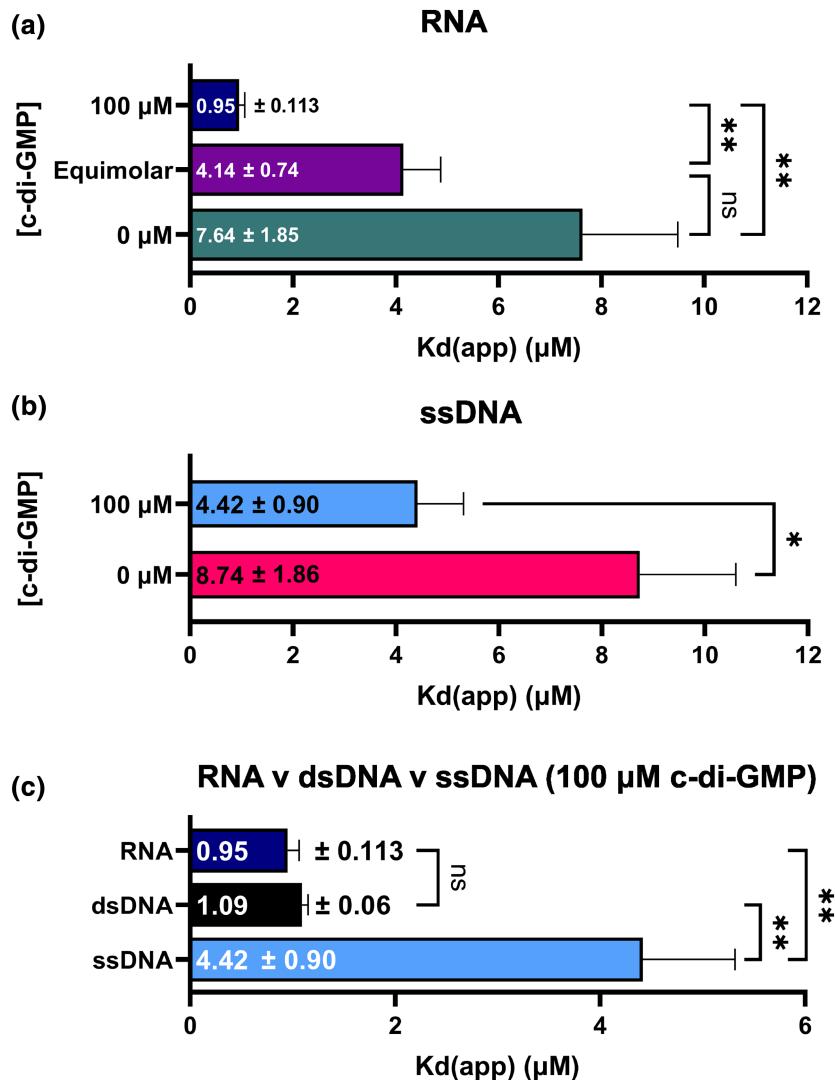
## 2.5 | Dissection of PlzA reveals the nucleic acid binding domain

The first discovered c-di-GMP binding receptors were the PilZ domain-containing proteins (Amikam & Galperin, 2006; Galperin & Chou, 2020; Ryjenkov et al., 2006). The PilZ domain consists of two conserved c-di-GMP binding motifs, RxxxR and [D/N]

ZSXXG (Amikam & Galperin, 2006; Cheang et al., 2019; Chou & Galperin, 2016; Ryjenkov et al., 2006). The recently solved crystal structure of *B. burgdorferi* PlzA revealed a unique dual-domain topology consisting of an amino-terminal PilZ-like domain, called PilZN3, which is connected to the carboxy-terminal PilZ domain via a linker domain that contains the RxxxR c-di-GMP binding motif (Singh et al., 2021). The first 141 amino acid residues make up the N-terminus of PlzA (PlzA<sub>NTD</sub>), while residues 142–261 make up the C-terminal (PlzA<sub>CTD</sub>) PilZ domain. Having determined that PlzA is a c-di-GMP-dependent DNA and RNA binding protein, we next sought to determine which domain of PlzA binds nucleic acid. To generate recombinant PlzA<sub>NTD</sub> and PlzA<sub>CTD</sub> domains, truncated *plzA* genes called *plzA*-NTD and *plzA*-CTD were cloned to encode the residues described above, which correspond to each respective domain (Figure 10a).

EMSA were performed with labeled *glpFKD*(-7/+35) DNA probe and increasing concentrations of PlzA<sub>NTD</sub> or PlzA<sub>CTD</sub>, with or without 100 μM c-di-GMP. PlzA<sub>NTD</sub> bound DNA independently of c-di-GMP, as supplementation with c-di-GMP did not affect binding (Figure 10b). PlzA<sub>CTD</sub> contains the motifs required for c-di-GMP binding, but the PlzA<sub>CTD</sub> domain did not bind to DNA with or without added c-di-GMP (Figure 10c). It was also determined that PlzA<sub>NTD</sub>

**FIGURE 9** c-di-GMP significantly impacts PlzA-nucleic acid binding and PlzA prefers dsDNA and RNA over ssDNA. (a) The  $K_{d(\text{app})}$  values from triplicate RNA EMSAs at each tested c-di-GMP concentration in Figure 8a were analyzed by a Welch ANOVA with Dunnett's T3 multiple comparisons test. (b) The  $K_{d(\text{app})}$  values from triplicate ssDNA EMSAs at the tested c-di-GMP concentrations in Figure 8c were analyzed by a Welch's t-test. (c) The  $K_{d(\text{app})}$  values from EMSAs with PlzA and each tested nucleic acid at 100  $\mu\text{M}$  c-di-GMP were compared via a Welch ANOVA with Dunnett's T3 multiple comparisons test. Bar graphs display the calculated  $K_{d(\text{app})} \pm$  the standard error of the mean (SEM). Adjusted  $p$ -values are indicated as follows:  $^{\text{ns}}p > 0.05$ ,  $^*p < 0.05$ , and  $^{**}p < 0.01$ .



could bind *glpFKD*(UTR) RNA with or without c-di-GMP, while PlzA<sub>CTD</sub> does not (Figure 10d,e, respectively).

We also performed the LC/MS-MS analysis on PlzA<sub>NTD</sub> and PlzA<sub>CTD</sub> recombinant proteins to determine if any di-nucleotides were present (Figure 11a). Co-purified c-di-GMP was detected in PlzA<sub>CTD</sub> but not PlzA<sub>NTD</sub>. The concentration of c-di-GMP present in recombinant PlzA<sub>CTD</sub> was determined as 704.29 nM. A total of 66.7  $\mu\text{M}$  of protein was sent for analysis indicating approximately 1.1% of PlzA<sub>CTD</sub> was bound with c-di-GMP. This indicates that PlzA<sub>CTD</sub> retained the ability to bind c-di-GMP but cannot bind nucleic acid.

To confirm that the truncated proteins were stably folded, circular dichroism (CD) was performed, and the CD spectra were obtained for PlzA<sub>WT</sub>, PlzA<sub>RD-RD</sub>, PlzA<sub>NTD</sub>, and PlzA<sub>CTD</sub> (Figure 11b). The CD results show that the mutated/truncated proteins retained stable structures matching that of PlzA<sub>WT</sub>. Therefore, the lack of nucleic acid binding by PlzA<sub>RD-RD</sub> and PlzA<sub>CTD</sub> was not due to improper folding. Secondary structure analysis was performed via the BeStSel server to further compare the recombinant proteins to the crystallized PlzA structure (Micsonai et al., 2015, 2018, 2022). All tested recombinant proteins show some differences from the calculated

secondary structures of the 7MIE PDB file. These deviations are primarily in the percentage of beta-sheet and turn secondary structure present. We note that the His-Tag was not cleaved prior to CD analysis of the recombinant proteins, and the resultant deviations could be due to the tag. The tag was considered in all calculations for CD. Overall, we can deduce that protein folding is not the cause of the lack of binding by PlzA<sub>RD-RD</sub> or PlzA<sub>CTD</sub>.

## 2.6 | Computational docking of PlzA-nucleic acid interactions

To gain a better understanding of the interactions between PlzA and DNA or RNA, we performed a computational docking analysis with the HDock server (Huang & Zou, 2014; Yan et al., 2020; Yan, Wen, et al., 2017; Yan, Zhang, et al., 2017). The *glpFKD*(-7/+35) DNA and *glpFKD*(UTR) RNA sequences were input as ligands, while the PlzA crystal structure (PDB ID: 7mie) was input as the receptor molecule. The modeling results indicate that interactions between PlzA and *glpFKD*(-7/+35) DNA are facilitated primarily through the

c-di-GMP ( $\mu\text{M}$ )	$K_{d(\text{app})}$ ( $\mu\text{M}$ ), 95% CI [LL, UL]	$B_{\text{max}}$ (% shifted), 95% CI [LL, UL]	Adj. R-squared
<i>glpFKD</i> (-7/+35) dsDNA			
100	1.09 [0.97, 1.23]	105.20 [102.20, 108.40]	0.986
50	1.25 [1.08, 1.45]	105.50 [101.50, 109.90]	0.981
25	1.33 [1.10, 1.59]	101.60 [96.58, 107.10]	0.971
10	2.81 [1.98, 4.02]	113.00 [98.79, 132.30]	0.940
Equimolar	4.22 [3.40, 5.26]	115.40 [104.40, 129.10]	0.983
0	7.86 [4.85, 14.06]	94.25 [71.72, 138.80]	0.950
<i>glpFKD</i> (UTR) RNA			
100	0.95 [0.73, 1.22]	102.6 [96.76, 109.20]	0.930
Equimolar	4.14 [2.79, 6.30]	106.7 [89.50, 132.60]	0.944
0	7.64 [4.71, 13.66]	87.73 [66.88, 128.80]	0.950
<i>glpF</i> ssDNA			
100	4.42 [2.94, 6.84]	102.80 [85.32, 129.90]	0.920
0	8.74 [5.67, 14.70]	82.04 [63.53, 116.90]	0.950

TABLE 1 Binding interaction summary of PlzA<sub>WT</sub> and the tested nucleic acids at various c-di-GMP concentrations.

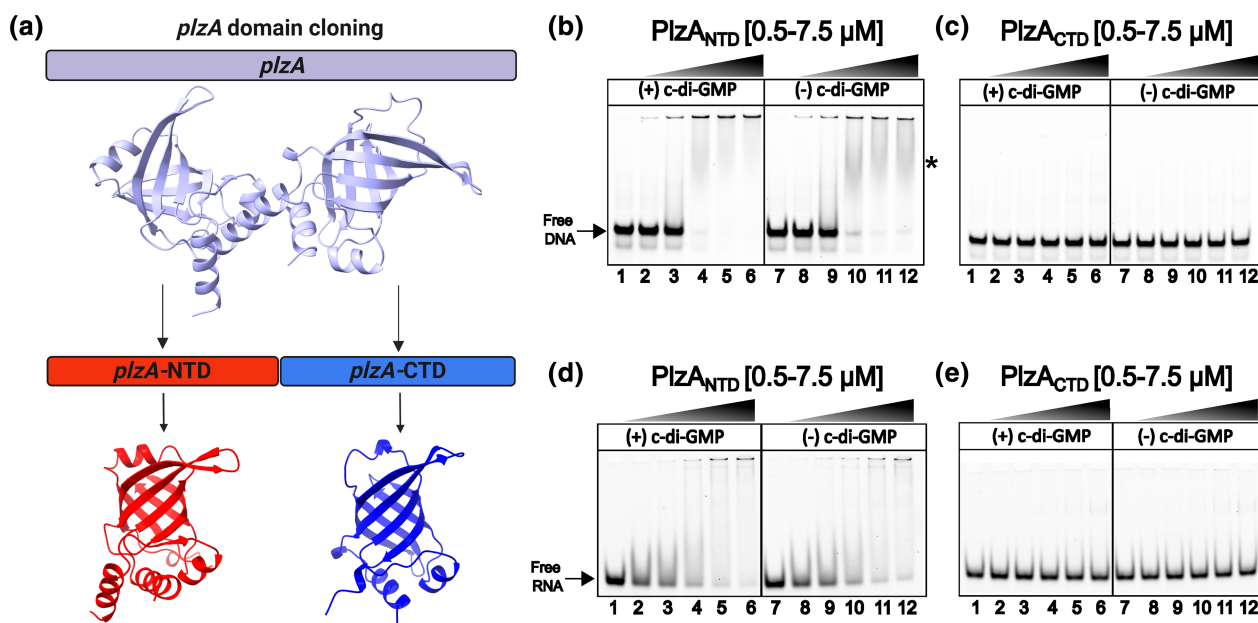
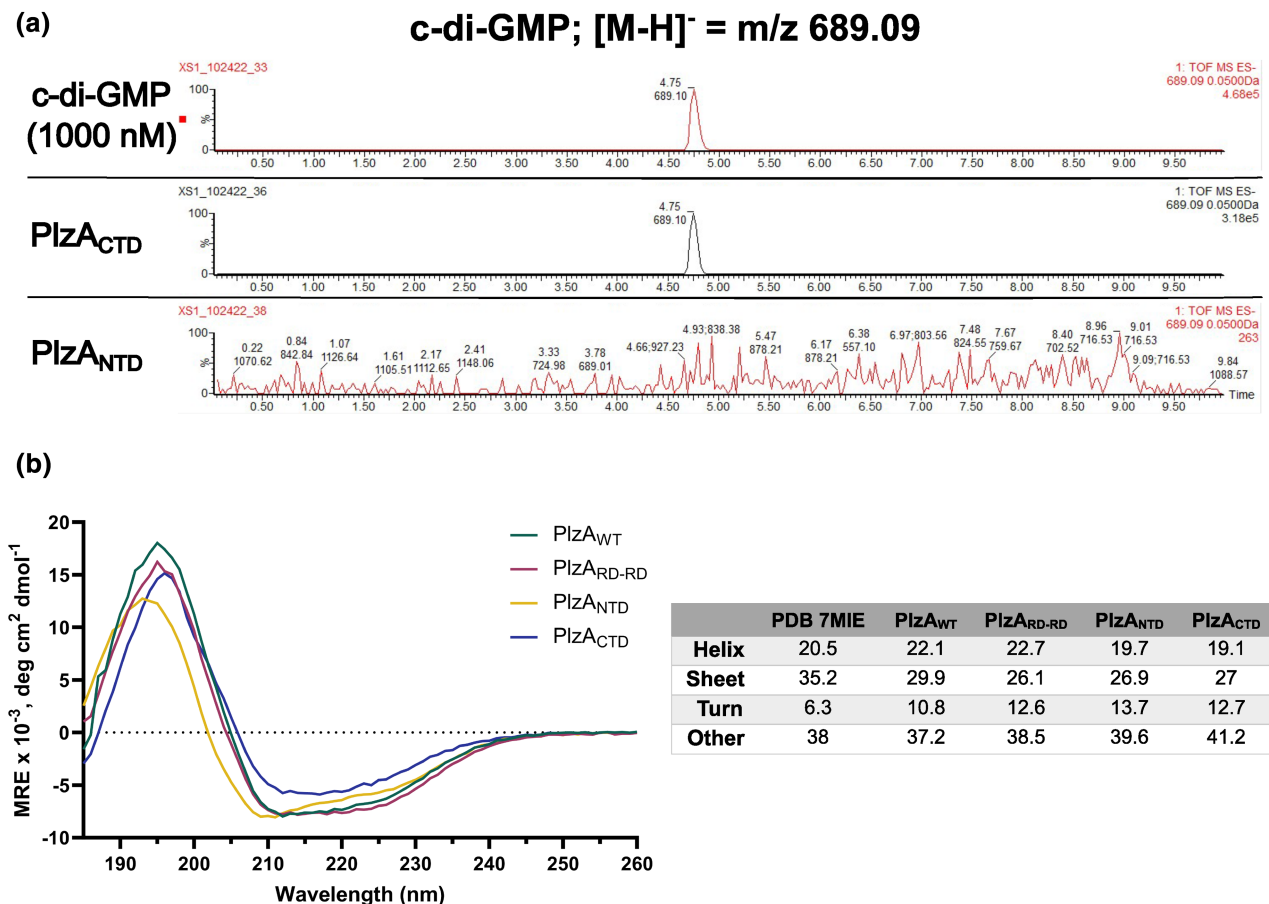


FIGURE 10 The N-terminal domain of PlzA is the nucleic acid binding domain. (a) The cloning strategy used to produce recombinant N (PlzA<sub>NTD</sub>) and C (PlzA<sub>CTD</sub>) terminal PlzA domains. The *plzA* gene portions corresponding to the N-terminus, *plzA*-NTD, and the C-terminus, *plzA*-CTD, were generated and cloned into an expression vector to produce recombinant PlzA<sub>NTD</sub> and PlzA<sub>CTD</sub> proteins. Gradient EMSAs were performed with increasing protein concentrations of PlzA<sub>NTD</sub> (b and d) or PlzA<sub>CTD</sub> (c and e) with (lanes 1–6) or without (lanes 7–12) 100  $\mu\text{M}$  c-di-GMP and 10 nM fluorescently labeled *glpFKD*(-7/35+) dsDNA (b and c) or *glpFKD*(UTR) RNA (d and e) probe. Lanes 1 and 7 are probe-only controls. Protein concentrations were as follows: Lanes 2 and 8: 0.5  $\mu\text{M}$ , Lanes 3 and 9: 1  $\mu\text{M}$ , Lanes 4 and 10: 2.5  $\mu\text{M}$ , Lanes 5 and 11: 5  $\mu\text{M}$ , Lanes 6 and 12: 7.5  $\mu\text{M}$ . SUPERase•In RNase inhibitor was supplemented to a final concentration of 2 U/ $\mu\text{L}$  in RNA EMSA mixtures. The asterisk indicates PlzA<sub>NTD</sub>-dsDNA shifts. Representative gels are shown from triplicate (PlzA<sub>NTD</sub>) or duplicate (PlzA<sub>CTD</sub>) EMSAs.

N-terminal domain (Figure 12a). In the representative docking data, beta-strands six and seven of the N-terminus are extended and protrude outward, intercalating a major groove of the DNA 5' to the protein docking site (Figure 12a top panel). Polar and positively charged amino acids, including N110 and K111, are located at the loop region where beta-strands 6 and 7 converge, with the potential to directly

interact with bases of the DNA (Rooman et al., 2002; Sathyapriya & Vishveshwara, 2004). Interactions with a minor groove of the DNA are predicted to occur through the loop region of beta-strands 2 and 3 and an unstructured linker region (Figure 12a bottom panel). Several positively charged residues, including arginine (R32 and R38) and lysine (K81), as well as an aromatic phenylalanine residue (F45), are



**FIGURE 11** Detection of c-di-GMP in recombinant PlzA<sub>NTD</sub> and PlzA<sub>CTD</sub> by LC-MS/MS and circular dichroism of proteins. (a) Recombinant PlzA<sub>NTD</sub> and PlzA<sub>CTD</sub> were sent off for mass spectrometry to detect the presence of c-di-GMP. Extracted ion chromatograms of the LC-MS/MS analysis are displayed. Chromatograms depict the control c-di-GMP standard at 1  $\mu$ M, recombinant PlzA<sub>CTD</sub>, and recombinant PlzA<sub>NTD</sub>. The LC-MS/MS analysis revealed that PlzA<sub>CTD</sub> co-purified with c-di-GMP, but PlzA<sub>NTD</sub> did not. The concentration of c-di-GMP in recombinant PlzA<sub>CTD</sub> was determined from a standard curve of c-di-GMP. PlzA<sub>CTD</sub> co-purified with 704.29 nM of c-di-GMP and approximately 1.1% of the protein was bound with c-di-GMP. The c-di-GMP standard chromatogram shown is the same as in Figure 3. (b) Circular dichroism spectra of recombinant PlzA<sub>WT</sub>, PlzA<sub>RD-RD</sub>, PlzA<sub>NTD</sub>, and PlzA<sub>CTD</sub> (see methods), and a summary table of the secondary structure analysis via BeStSel of recombinant proteins versus the PlzA PDB file 7MIE. CD spectra were derived from averaging the CD results from two different recombinant protein preparations for each protein tested. A buffer only control was performed and subtracted from the averaged measured recombinant protein CD spectra.

predicted to directly interact with the minor groove and backbone of the DNA. An additional lysine residue K87, which is in the unstructured region, protrudes and interacts directly with bases of another major groove of *glpFKD*(-7/+35). No residues of the C-terminal domain are predicted to interact directly with the DNA; however, four residues are interfacing the DNA (K161, I213, D258, and N261). Residue K161 hovers over the DNA backbone potentially interacting nonspecifically via electrostatic interactions. We note that the docking analysis produced several potential models that differed in the location of where residues interact with either the minor or major groove. The model presented is the highest-ranking model. Overall, the computational docking data supports our EMSA data showing that PlzA<sub>NTD</sub> binds DNA while PlzA<sub>CTD</sub> does not (Figures 10b,c) and that PlzA interacts predominately with the major groove of DNA (Figure 5).

The docking analysis was also performed with PlzA<sub>WT</sub> and *glpFKD*(UTR) RNA (Figure 12b). Again, the N-terminal domain of PlzA

facilitates most of the interactions. Similar regions of the protein that interacted with dsDNA are implicated in the interaction with RNA including the residues of the loop region of beta-strands 6 and 7 (K111 and Y113), the loop region of beta-strands 2 and 3 (R38, Y42, and F45) and the unstructured linker region (R32, D85, K87, F92, and F95). Unlike the docking model with dsDNA, the PlzA-RNA docking model indicates more involvement of the C-terminal domain in RNA binding. Several residues of alpha-helices 5 (D155, R158, K159, and K161) and 6 (D258 and Y259) in the C-terminal domain of PlzA, are predicted to interact with RNA. Although our EMSA results show that PlzA<sub>CTD</sub> does not bind any tested nucleic acids, the docking results indicate it could help stabilize PlzA<sub>NTD</sub>-nucleic acid interactions or could be involved in target recognition. Guided by the docking data, we are in the process of generating site-directed PlzA mutant proteins that will explore residues predicted to be involved in nucleic-acid binding.

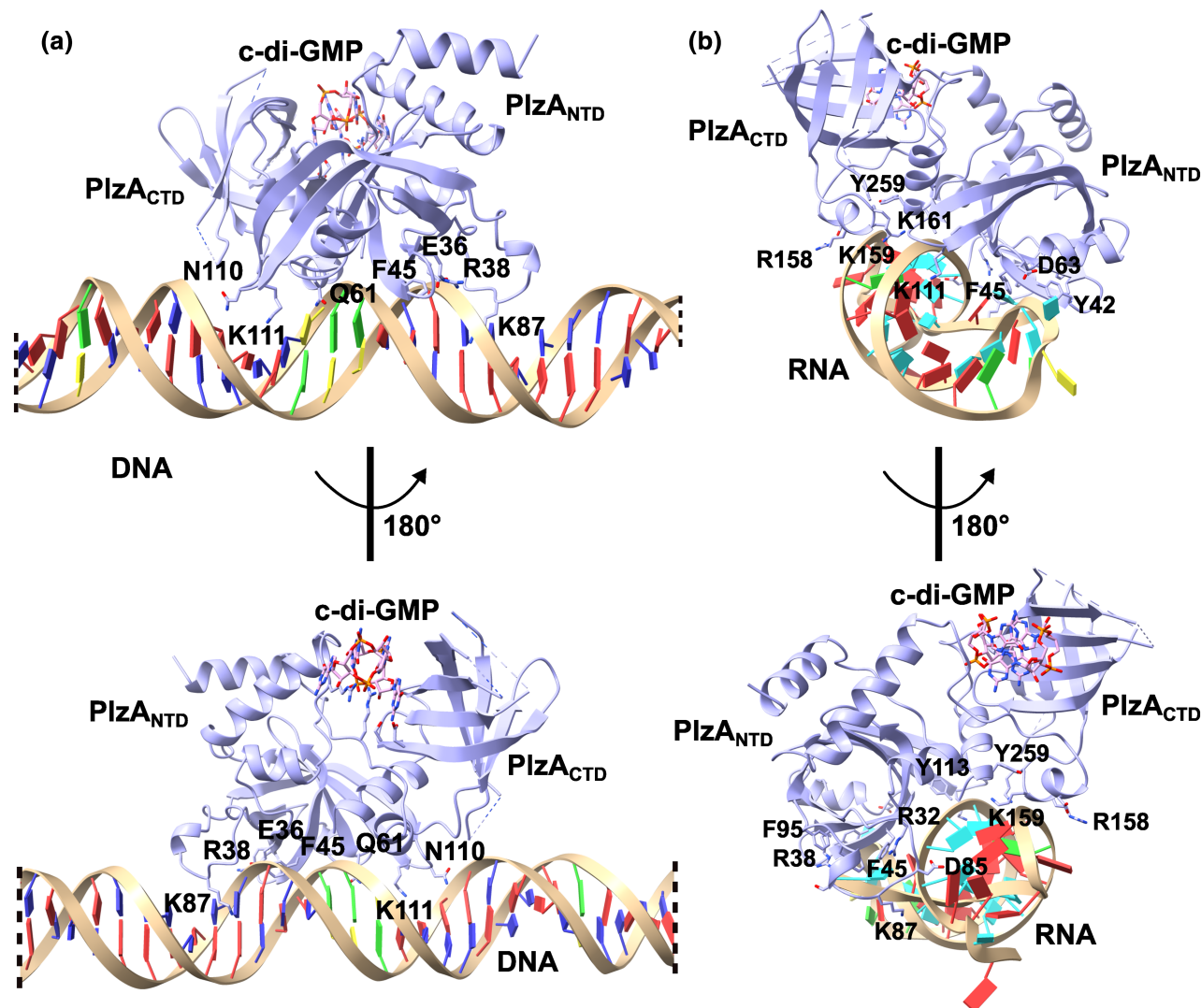


**FIGURE 12** Computational docking analysis of PlzA with *glp* DNA and RNA. Computational docking was performed using the HDock server with PlzA and either (a) the 42 bp *glpFKD*(-7/+35) dsDNA or (b) the *glpFKD*(UTR) RNA sequence. In (a) only 26 of 42 bp of the *glpFKD*(-7/+35) sequence is shown. The dashed lines represent where bases were left out of the figure to zoom in on the protein-DNA interactions. The dsDNA model was linear, and removal of the bases has no impact on the interpretation of the data. The top predicted model from each computation is shown. The HDock docking and confidence scores for each model were -210.60 and 0.77 for PlzA-*glp* DNA, and -280.71 and 0.93 for PlzA-*glp* RNA, respectively. The protein is rotated 180° from the top to the bottom panels. Select amino acid residues that interface the nucleic acids are labeled.

Computational docking was attempted with PlzA and *ssglpF*, but the HDock server could not complete the analysis. Given that PlzA bound dsDNA and RNA better than ssDNA, it is interesting to note that the computational modeling predicts the RNA to fold into a double stranded secondary structure. Combined with our EMSA data, this suggests that PlzA could have a preference towards double stranded nucleic acids and/or secondary structures.

### 3 | DISCUSSION

Cyclic-di-GMP has wide-ranging effects on many bacterial processes. The responses to c-di-GMP are commonly mediated through c-di-GMP binding effector proteins. PlzA is the only chromosomally

and universally encoded c-di-GMP binding protein of the Lyme disease spirochetes. It has been shown to be crucial for borrelial infection processes and in the regulation of the metabolism of alternative carbon sources during colonization of vector ticks (Groshong et al., 2021; He et al., 2014; Mallory et al., 2016; Pappas et al., 2011; Pitzer et al., 2011; Zhang et al., 2018). Despite its singularity and importance to *B. burgdorferi*, little was previously known about the biochemical functions of PlzA outside of binding c-di-GMP. Here, we provide evidence that PlzA is a novel c-di-GMP-dependent nucleic acid-binding protein.

While PlzA lacks an obvious canonical DNA binding motif, we hypothesized that PlzA might be a nucleic acid binding protein, given its role in the regulation of the *glpFKD* operon. Binding was only observed by the wild-type PlzA protein but not the mutant,

PlzA<sub>RD-RD</sub>, which is incapable of binding c-di-GMP. It has previously been shown that structural rearrangements are induced upon the binding of c-di-GMP to PlzA (Groshong et al., 2021; Mallory et al., 2016). Without bound c-di-GMP, the N- and C-terminal domains of PlzA can flex on an unstructured linker, potentially inhibiting the stable interactions that are necessary for DNA and RNA binding. This hypothesis is supported by the fact that crystallization of PlzA was only achieved when saturated with c-di-GMP (Singh et al., 2021). We surmise that binding of c-di-GMP to the C-terminal PilZ domain results in a change of PlzA into a more rigid structure, which permits nucleic acid binding through residues of the N-terminal domain.

We identified the N-terminal domain of PlzA as the nucleic acid binding domain and that PlzA<sub>NTD</sub> bound DNA independently of c-di-GMP. In contrast, the C-terminal domain, PlzA<sub>CTD</sub>, did not bind any tested nucleic acids, although it still bound c-di-GMP. Although PlzA<sub>NTD</sub> can interact with nucleic acids, these interactions were not as strong as PlzA<sub>WT</sub>. Binding of nucleic acid by PlzA<sub>NTD</sub> resulted in smeared shifts that lacked defined bands. This suggests instability of the PlzA<sub>NTD</sub>-nucleic acid complexes resulting in dissociation of the complexes during electrophoresis. Noting that binding of c-di-GMP appears to stiffen interactions between the N- and C-terminal domains, we hypothesize the C-terminal domain may stabilize the interactions of PlzA<sub>NTD</sub> with nucleic acids when c-di-GMP is bound. On the other hand, we posit that the flexibility of apo-PlzA results in the C-terminal domain disrupting the ability of the N-terminal domain to stably bind DNA. Although the N- and C-terminal PlzA domains are similar, structural comparisons of PlzA<sub>NTD</sub> and PlzA<sub>CTD</sub> reveal distinct differences (Figure 10a). The N-terminus of PlzA<sub>NTD</sub> contains an alpha-helix that is absent in the N-terminus of PlzA<sub>CTD</sub>. Additionally, an alpha-helix is present at the beta-barrel pore of PlzA<sub>NTD</sub> but not in the PlzA<sub>CTD</sub>. These differences suggest distinct roles in PlzA-nucleic acid binding dynamics. We are currently exploring the sequence motifs recognized by PlzA and the exact amino acid residues involved in nucleic acid binding.

Previous studies found that PlzA is a monomer in solution regardless of c-di-GMP (Mallory et al., 2016). While many DNA-binding proteins bind DNA as dimers, alternative binding models exist (Kim & Little, 1992; Kohler et al., 1999). It has been shown that some proteins bind sequentially as monomers which then multimerize on the DNA via protein-protein interactions, such as some members of the Leucine zipper and helix-loop-helix zipper families, the LexA repressor of *E. coli*, and BpaB of *B. burgdorferi* (Burns et al., 2010; Kim & Little, 1992; Kohler et al., 1999). Our studies revealed that increasing c-di-GMP and PlzA<sub>WT</sub> concentrations resulted in progressively slower migration of PlzA-*glpFKD*(-7/+35) DNA complexes. The decreases in the migration of the complexes that are observed with increasing protein concentration may indicate a stoichiometry that is not 1:1, or the observed smearing may be the result of dynamic equilibrium of the complexes in the gels during electrophoresis (Fried, 1989; Fried & Crothers, 1981). While increasing c-di-GMP enhances PlzA binding, there could be a threshold where too much c-di-GMP is inhibitory and causes

dissociation of PlzA from nucleic acids. A dimerization or protein-protein interaction residue/motif/domain remains to be identified in PlzA, and work is ongoing to address the DNA-binding mode and stoichiometry of PlzA-nucleic acid complexes.

We also observed probe signal in the gel wells at high protein and c-di-GMP concentrations. This could be due to protein aggregation. Rather than simply being a negative consequence of environmental stress, recent studies indicate a role for protein aggregation in regulation. Specifically, certain conditions can induce a protein to aggregate, and thus be sequestered, altering gene expression to permit bacterial adaptation to a specific environment (Schramm et al., 2019). Whether high levels of c-di-GMP promote such processes remains to be tested, but c-di-GMP levels certainly alter PlzA binding affinity.

Our study sought to identify if PlzA can bind nucleic acids and what role c-di-GMP plays in that function. The data are conclusive that PlzA indeed binds DNA, both double and single-stranded, and RNA, with a preference for dsDNA and RNA. PlzA also displayed higher affinity for certain nucleic acid types over others, and PlzA-*glp* DNA binding was competed away by specific competitors. Further, the nucleic acid binding at the *glpFKD* locus by PlzA is dependent on c-di-GMP. A caveat of the data is that the calculated dissociation constants for PlzA-nucleic acids are lower than typically observed for protein-nucleic acid interactions. The higher dissociation constants could be attributed to our method of choice, EMSA, as some potential dissociation and protein aggregation were observed. Attempts were made with various alterations aimed to improve the stability of the complexes during electrophoresis, such as altering the gel percentage, pH of the running buffer, salt/ion concentrations of the reaction buffer, and addition of detergents to the reaction (Hellman & Fried, 2007). Altering the pH of the running buffer to 8.0 decreased the aggregation in the wells but smearing still occurred at higher protein and c-di-GMP concentrations (data not shown). The experimental conditions presented and reported here yielded the most consistent results.

PlzA bound to a sequence adjacent to the promoter and extending 35 bp into the 5' UTR of *glpF*. This site has been shown to positively affect *glpFKD* transcript levels and is a site where two other borrelial regulators, SpoVG and BadR, also bind (Grove et al., 2017; Savage et al., 2018; Saylor et al., 2023; Zhang et al., 2024). BadR, the *Borrelia* Host Adaptation Regulator, has recently been identified as a repressor of *glpFKD*, while PlzA has previously been shown to exert both positive and negative effects on *glpFKD*, at high and low levels of c-di-GMP, respectively (Zhang et al., 2018, 2024). Although SpoVG can bind the DNA and RNA of *glpFKD*, the transcriptional consequences of these interactions are unknown (Savage et al., 2018; Saylor et al., 2023). How these proteins work in tandem to regulate glycerol catabolism is currently being investigated. Multi-layered regulation of glycerol catabolism is found in other bacteria, indicating this is not a phenomenon unique to *Borrelia* (Bong et al., 2019).

Our data show that PlzA is a DNA and RNA binding protein that is c-di-GMP dependent. Obvious questions that remain are what sequence motif(s) PlzA recognizes and what additional binding sites

may exist in the *B. burgdorferi* genome. Our studies were unable to identify an obvious sequence motif in the *glpFKD* intergenic region but were able to identify that PlzA interacts mainly with the major groove of DNA. We also saw a preference of PlzA for longer sequences and A-T rich sequences. The lesser affinity for shorter sequences could indicate that PlzA might recognize structured nucleic acids, as shorter DNA/RNA are less likely to form structured conformations. Therefore, it cannot be ruled out that PlzA may recognize gene targets in a sequence independent manner. Given that poly-dl-dC did not abolish binding and that some mutant competitors did not compete as well as others, PlzA likely exhibits preferential affinity to certain nucleic acids. Whether the preferential affinity is due to a sequence motif or structural motifs, remains to be determined. What is clear, from multiple studies, is that the cellular effects exerted by PlzA are specific.

A logical step to address these questions is to perform chromatin immunoprecipitation with sequencing (ChIP-Seq). Given that PlzA binding is reliant on an effector molecule, *c*-di-GMP, there are some caveats in performing this assay at this stage. First, the activating stimulus for the Hk1/Rrp1 pathway is currently unknown. As a result, it is unknown how levels of *c*-di-GMP fluctuate in culture medium and across growth phases, and therefore how much *c*-di-GMP is produced in a bacterial cell at a given time. This can affect the ability to obtain consistent ChIP results. The tendency of protein to occupy each site will likely vary with culture conditions. Therefore, optimal experimental conditions must be determined before obtaining and drawing conclusions about PlzA binding sites derived from ChIP experiments.

Next, as mentioned above, two other proteins have been found to bind the same site within *glpFKD*, SpoVG and BadR (Savage et al., 2018; Saylor et al., 2023; Zhang et al., 2024). Competition between these proteins could also impact the ChIP data. Additionally, the molecular consequence of nucleic acid binding remains to be determined. We are actively working to address these questions by characterizing several PlzA site-direct mutant proteins incapable of binding nucleic acids to determine impacts on *B. burgdorferi* physiology and gene regulation. Such work will also aid in identifying targets of PlzA regulation to better guide the identification of additional binding sites.

During the preparation of this manuscript, Van Gundy et al. (2023) published a report identifying RNA chaperone activity by PlzA. The authors concluded that this activity is independent of *c*-di-GMP, which deviates from our results showing that *c*-di-GMP is required for nucleic acid binding. Those authors acknowledged this and suggested that differences in methodologies and conditions might have contributed to the differences in observed results. Some of these differences include using non-borrelial derived RNAs, a different PlzA site-mutant, equimolar concentrations of *c*-di-GMP, and filter binding assays used to calculate dissociation constants.

We chose to evaluate saturating *c*-di-GMP concentrations to evaluate the maximal nucleic acid binding activity of holo-PlzA and mitigate potential variability in the calculated apparent  $K_D$  values. Van Gundy et al. did not assess whether their PlzA protein

preparations co-purified with *c*-di-GMP, which could have contributed to their observed binding by apo-PlzA. Unlike their study, we did not observe binding by the PlzA<sub>RD-RD</sub> mutant, which cannot bind *c*-di-GMP, under any tested condition. Given the stabilizing effect *c*-di-GMP binding has on the structure of PlzA (only the holo form was able to be crystallized), the ability of their mutant and apo-PlzA to bind RNA merits further mechanistic investigation. Lastly, the goals for our studies differed greatly as they sought to study RNA chaperone activity, while we set out to investigate the ability of PlzA to bind nucleic acids. Our two studies, however, corroborate that PlzA can bind RNA and suggest that this function plays a role in regulating borrelial gene expression. We agree that further investigation is required to unravel the molecular mechanisms of PlzA interactions with nucleic acids, and the roles that those interactions play in gene regulation in this important pathogen.

It is known that the affinity and specificity of proteins for target nucleic acids are impacted by co-effectors (Carey, 2022). We observed that adding exogenous *c*-di-GMP increased binding affinity of PlzA for *glp*-derived DNA and RNA. The localization of *c*-di-GMP and associated proteins in *B. burgdorferi* is currently unknown. Whether the *c*-di-GMP signaling network is global or localized will be key to understanding how *c*-di-GMP induces PlzA effector functions. This is actively being investigated by our laboratory. Studies in other bacteria with multiple PilZ domain proteins have suggested that the differential affinity of the various PilZ receptors for *c*-di-GMP sequentially regulates the processes that respond to *c*-di-GMP (Junkermeier & Hengge, 2023; Pultz et al., 2012). Given that PlzA is the only PilZ domain protein in most *B. burgdorferi* isolates, an alternative to this could be that cellular levels of *c*-di-GMP alter the affinity and/or specificity of PlzA.

We propose a model in which *c*-di-GMP availability alters the functionality of PlzA, and thus, the targets regulated by PlzA could depend on the *c*-di-GMP levels available at different stages of the enzootic life cycle (Figure 13). During vertebrate infection, no *c*-di-GMP is produced, favoring apo-PlzA functions such as RNA chaperone activity (Van Gundy et al., 2023). When *c*-di-GMP is present, holo-PlzA can also anneal RNAs and potentially interact with RNAP (Grassmann et al., 2023; Van Gundy et al., 2023). At lower levels of *c*-di-GMP, PlzA nucleic-acid binding affinity is low for target loci. As *c*-di-GMP levels increase further, binding affinity for target nucleic acids is increased and potential multimerization of PlzA molecules on DNA could occur.

In conclusion, PlzA is a *c*-di-GMP-dependent nucleic acid-binding protein. While other *c*-di-GMP binding receptors have been identified as DNA-binding proteins, PlzA is the first that has been demonstrated to also bind RNA, thus expanding the functional diversity of *c*-di-GMP binding proteins. Given that PlzA can bind to both DNA and RNA, it could have a role in coordinating transcriptional complexes, and it supports the notion that PlzA can interact with RNAP (Grassmann et al., 2023). Our study examined PlzA nucleic acid binding at a locus known to be affected by PlzA, the *glpFKD* catabolism operon, but sites of higher affinity could exist. Our work identifying PlzA as a novel nucleic acid-binding protein provides a basis for its

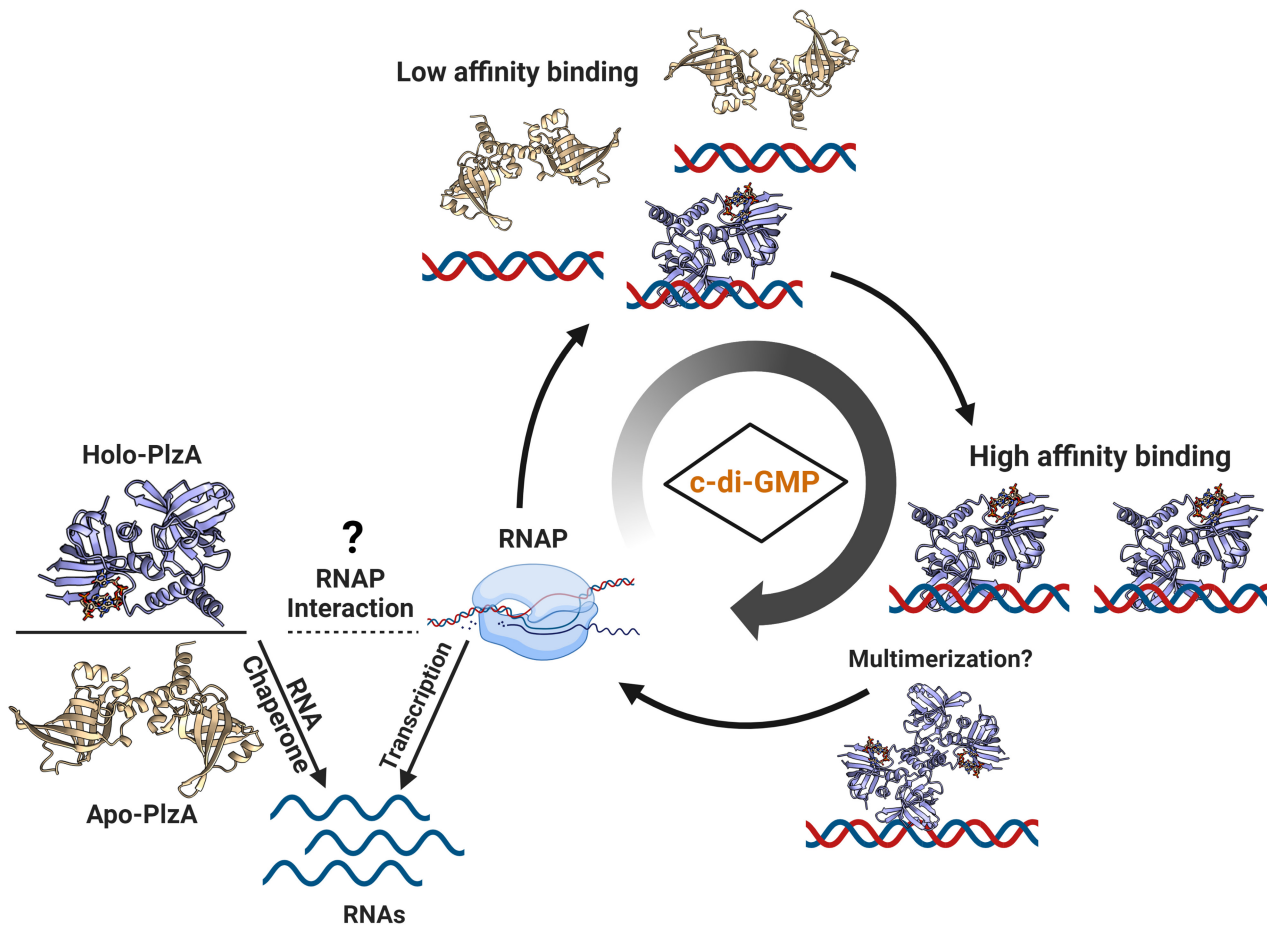


**FIGURE 13** Model depicting the modulation of PlzA function by levels of c-di-GMP. Apo and holo-PlzA are hypothesized to have distinct functions in the vertebrate and tick hosts respectively. Recent studies identified PlzA RNA chaperone activity that is c-di-GMP independent (Van Gundy et al., 2023). In environments with no c-di-GMP, such as the vertebrate host, apo-PlzA engages in RNA chaperone activity to modulate gene expression required for survival in the vertebrate host. The phosphodiesterases PdeA and PdeB are likely to be highly active upon transmission and into vertebrate infection, lowering c-di-GMP levels and facilitating apo-PlzA functions (Groshong et al., 2021; Novak et al., 2014; Pitzer et al., 2011; Sultan et al., 2010, 2011). Phosphodiesterase activity is likely to occur at all stages to regulate c-di-GMP levels and indirectly, PlzA function. When Hk1 is activated (signal unknown), Rrp1 is phosphorylated and produces c-di-GMP. Holo-PlzA can also engage in RNA chaperone activity by annealing RNAs, and potentially interact with RNAP (Grassmann et al., 2023; Van Gundy et al., 2023). We propose that levels of c-di-GMP impact the specific genes regulated by PlzA through altering nucleic acid binding affinity. At lower c-di-GMP levels, few holo-PlzA monomers exist resulting in weak PlzA binding affinity for certain target loci. As levels of c-di-GMP increase, more holo-PlzA molecules bind target genes with higher affinity, and PlzA could potentially multimerize on DNA.

functional mechanism. This will further inform our understanding of how *B. burgdorferi* regulates gene expression in response to environmental cues and help unravel the PlzA regulon.

## 4 | MATERIALS AND METHODS

### 4.1 | Routine manipulations and molecular cloning

Oligonucleotides used in this study are listed in Table 2 and were ordered from Integrated DNA Technologies (IDT). *B. burgdorferi* genomic DNA was purified utilizing the E.Z.N.A Tissue DNA kit (OMEGA). Standard and high-fidelity PCR were performed with 2X DreamTaq Green PCR Master Mix (Thermo Scientific) or Q5 High-Fidelity 2X Master Mix (NEB), respectively. Plasmids were isolated

using QIAprep Spin Miniprep kits (Qiagen) according to the Miraprep protocol (Pronobis et al., 2016). All plasmid constructs were transformed into chemically competent *E. coli* Top10 (Invitrogen) or DH5 $\alpha$  (Invitrogen) strains for cloning and plasmid maintenance. Positive clones were identified by colony PCR screening with the appropriate primer sets, and DNA sequencing was performed by Eurofins Genomics LLC (Louisville, KY).

### 4.2 | Plasmid construction

The wild-type (WT) *plzA* gene from *B. burgdorferi* strain B31, was cloned between the NdeI/XhoI sites of pET28a(+) and thus fused in-frame with an amino-terminal 6xHis-tag. Truncated *plzA* genes, named *plzA*-NTD and *plzA*-CTD encoding the N-terminal (residues

TABLE 2 Oligonucleotides used in this study.

Target	Name and sequence (5' → 3')	Size (bp)
Cloning and sequencing primers		
<i>plzA</i>	<i>plzA</i> F: GGCAGCC <b><u>ATATG</u></b> CTTTTATCTAGAAAAATAAGAGATTATG <i>plzA</i> R: GTGGT <b><u>GCTCGAG</u></b> TAAATTGAAATAATCATGGATCAAC	786
MCS pET28a(+): <i>plzA</i>	T7 F: TAATACGACTCACTATAGGG T7 R: TAGTTATTGCTCAGCGGTGG	1026
pCR 2.1 TA clones	M13 F: GTAAAACGACGGCCAG M13 R: CAGGAAACAGCTATGAC	N/A
<i>plzA</i> -NTD	<i>plzA</i> 1F: ATGCTTTTATCTAGAAAAATAAGAGATTATG <i>plzA</i> N R: T TACTGATTTTGCCCAAGCTTTAAATC	435
<i>plzA</i> -CTD	<i>plzA</i> C F: ATGGATTTAAAGCTTGGGCAA <i>plzA</i> 1R: ATTGAAATAATCATGGATCAACATAGTATAC	378
Site-directed mutagenesis primers		
<i>plzA</i> R145-149D	<i>plzA</i> -mut F: AATCAGGACATTCATGAGGACATTATTATCGATAAAGATTCTATTAG <i>plzA</i> -mut R: GTCCTCATGAATGTCCTGATTTTGCCCAAGCTTTAAATCAAGAAGCTTTCC	786
EMSA probes, competitors, and primers		
<i>glpFKD</i> (-219)	M13 F: GTAAAACGACGGCCAG M13 R 5' IRD800CW or unlabeled: CAGGAAACAGCTATGAC	654
<i>glpFKD</i> (-7/+35)	<i>glpF</i> F IRD800: ATTAAATATAATTTTAATAAGGCTTTTATTAGAAAAATTAAT <i>glpF</i> R: ATTAATTTTCTAATAAAAAGCCTTATTAATAATATATTAAT	42
<i>ssglpF</i>	<i>glpF</i> F IRD800: ATTAAATATAATTTTAATAAGGCTTTTATTAGAAAAATTAAT	42
<i>glpFKD</i> (UTR) RNA	<i>glpF</i> RNA 5' Alexa488: AUAAUUUUUAAUAAGGCUUUUUAUUAGAAAAUUAAU	35
pCR 2.1 competitor	M13 F: GTAAAACGACGGCCAG M13 R: CAGGAAACAGCTATGAC	210

Note: Bolded and underlined nucleotides indicate restriction enzyme sites.

1–141) and C-terminal (residues 142–261) domains of PlzA, respectively, were generated via gene synthesis and cloned to produce 6xHis-tagged proteins by Genscript (Piscataway, NJ). Briefly, the synthesized truncations were cloned into the pET28b(+) vector with *plzA*-NTD cloned between the BamHI/NotI sites producing an amino-terminal 6xHis-tag fusion, while *plzA* CTD was cloned between the NcoI/XhoI sites producing a carboxy-terminal 6xHis-tag fusion.

### 4.3 | Generation of the site-directed PlzA R145D-R149D mutant

Site-directed mutagenesis by overlap extension PCR was used to generate a PlzA mutant that cannot bind c-di-GMP. Two-point mutations were introduced into a pTrcHis TOPO (Invitrogen) construct containing the *plzA* gene. The successful introduction of the mutations was confirmed by DNA sequencing. The site-directed PlzA double mutant is denoted as PlzA<sub>RD-RD</sub>. The oligonucleotide primers used for site-directed mutagenesis are listed in Table 2.

### 4.4 | Recombinant protein overexpression and purification

For recombinant protein expression, *E. coli* Rosetta 2(DE3)(pLysS) (Novagen) chemically competent cells were used for PlzA<sub>WT</sub>,

PlzA<sub>RD-RD</sub>, and N-terminal PlzA domain (PlzA<sub>NTD</sub>), while One Shot BL21 Star (DE3) cells were used for the C-terminal PlzA domain (PlzA<sub>CTD</sub>). Overnight bacterial cultures were diluted 1:100 into Super broth (tryptone 32g, yeast extract 20g, NaCl 5g/L) supplemented with the appropriate antibiotics (kanamycin-50 μg/mL, carbenicillin-100 μg/mL, and/or chloramphenicol-30 μg/mL). The cultures were allowed to grow to an OD<sub>600</sub> of 0.5–1.0 and protein expression was subsequently induced by the addition of 0.25 mM (PlzA<sub>NTD</sub> only) or 0.5 mM isopropyl-β-D-thiogalactopyranoside (IPTG). Induced cultures were incubated at either 37°C for 3–4 h (PlzA<sub>WT</sub> and PlzA<sub>CTD</sub>), 29°C for 4–6 h (PlzA<sub>WT</sub>), or overnight at room temperature (PlzA<sub>RD-RD</sub> and PlzA<sub>NTD</sub>). The cells were harvested by centrifugation at 5400 × g for 30 min at 4°C, and the cell pellets were frozen at –80°C until protein purification.

For protein extraction, cell pellets were thawed on ice and resuspended in equilibration buffer (20 mM sodium phosphate, 300 mM NaCl, 10 mM imidazole, pH 8.0) and lysed via sonication. Lysates were clarified by centrifugation at 23,700 × g for 20 min at 4°C, and the supernatant was retained. When further clarification was required due to lysate viscosity, the supernatants were passed through a sterile 0.22 μm Millex-GS Syringe Filter Unit (MilliporeSigma). Protein purification was performed via column affinity chromatography using either HisPur Ni-NTA resin (Thermo Scientific) or the Magne-His purification system (Promega Corporation) for PlzA<sub>RD-RD</sub> per manufacturer protocol. Eluted protein solutions were dialyzed overnight into either EMSA

buffer (50 mM Tris-HCl [pH 7.5], 50 mM KCl, 1 mM dithiothreitol (DTT), 1 mM ethylenediaminetetraacetic acid (EDTA) [pH 8.0], 1 mM phenylmethanesulfonyl fluoride (PMSF), 10% glycerol (v/v), and 0.01% Tween-20) or 20 mM sodium phosphate, pH 7.2. The dialyzed proteins were then concentrated using Amicon Ultra 3K (PlzA<sub>N</sub> and PlzA<sub>C</sub>) or 10K (PlzA<sub>WT</sub> and PlzA<sub>RD-RD</sub>) centrifugal filter units (MilliporeSigma). Aliquots of dialyzed proteins were assessed for purity by SDS-PAGE and Coomassie brilliant blue staining. Final recombinant protein concentrations were determined using Quick Start Bradford Protein Assays (Bio-Rad) with bovine serum albumin as the reference protein for standard curves. Purified protein aliquots were stored at -80°C.

#### 4.5 | Nucleic acid fragments design and generation

All probe sequences were derived from the genomic sequence of *B. burgdorferi* type strain B31, and the corresponding primers are reported in Table 2 (Casjens et al., 2000; Fraser et al., 1997). Large and small DNA substrates were used in this study. Larger fluorescently tagged fragments >60 bp were generated by PCR amplification of the target sequences from B31 genomic DNA and subsequent cloning into the pCR 2.1 TA vector (Invitrogen) following TOPO TA protocols. Subsequently, target-specific or M13 F and R IRDye 800-labeled primers were used for PCR of the plasmid templates to produce labeled DNA fragments for binding studies. All PCR-generated probes were treated with exonuclease I (NEB) according to the manufacturer's protocol to remove single-stranded DNA, followed by ethanol precipitation. The DNA was resuspended in molecular-grade water (Ambion) and quantified by Nanodrop UV spectrometry.

Smaller probes <60 bp long were produced by annealing complementary unlabeled and IRDye 800-labeled oligonucleotides at equimolar concentrations at 95°C for 5 min and were gradually cooled overnight at RT. The same annealing procedure was done for unlabeled competitors. All probes and competitors were aliquoted and stored at -20°C until further use. Unlabeled and 5' IRDye 800 (LI-COR Biosciences) labeled oligonucleotides were synthesized by IDT. Alexa Fluor 488 conjugated RNA probes corresponding to the transcribed regions of the respective DNA probes were also synthesized by IDT.

#### 4.6 | Electrophoretic mobility shift assays (EMSA)

EMSA reactions were performed in EMSA buffer at RT with a final concentration of dsDNA probe of 10 nM or RNA probe of either 10 nM or 50 nM. EMSA reaction mixtures were supplemented with 3'5' c-di-GMP (Sigma-Aldrich) at various concentrations ranging from 0 to 100 μM. c-di-GMP was not added to the gel or running buffer. Experiments using equimolar concentrations of c-di-GMP are relative to the final protein concentration in the reaction. Proteins were co-incubated with c-di-GMP for 5 min before the addition of any nucleic acids. Prior to the addition of labeled

probe, the non-specific competitor poly-dl-dC (Roche) was added to the EMSA reactions at a final concentration of 2.5 ng/μL, and the reaction mix was allowed to incubate another 5 min (Larouche et al., 1996). Labeled probes were added last, and the reactions were subsequently incubated for an additional 10 min prior to loading onto gels. Competition EMSAs were conducted similarly but with the unlabeled, specific competitor added after poly-dl-dC and then allowed to incubate 5 min with the reaction prior to the addition of the labeled probe. Regarding RNA EMSAs, when RNase contamination was evident in recombinant protein preparations, RiboGuard (Lucigen) or SUPERase•In (Ambion) RNase inhibitor was added to the EMSA mixtures before the addition of RNA to a final concentration of 4 U/μL and 2 U/μL respectively to inhibit RNase activity. The final reaction volume was 10 μL prior to the addition of loading dye.

For visualization during electrophoresis, 2 μL of EMSA loading dye (0.8 mg/mL Orange G, 15 mg/mL Ficoll 400) was added to each reaction prior to gel loading. Novex TBE 6 or 10% gels (Invitrogen) were pre-run in 0.5x TBE running buffer (pH ~8.4 ± 0.5), at 100 V for a minimum of 30 min. Due to the complexes of the larger *gfp-FKD(-219)* probe and higher concentrations of PlzA not exiting the well, the pH of the running buffer was adjusted to a pH of 8.0 immediately prior to electrophoresis, which allowed the complexes to enter the gel matrix. The pH was not adjusted for EMSAs using nucleic acid fragments <60 bp as complexes readily exited the well at the standard pH of 0.5x TBE running buffer. The entire reaction mixture was then loaded onto the pre-run gels and resolved at 100 V for 60–90 min at RT. EMSA images were acquired with a ChemiDoc Imaging System (Bio-Rad).

#### 4.7 | Densitometry and statistics

Densitometry of EMSAs was performed using Image Lab 6.1 (Bio-Rad) software. Analyses were performed on triplicate EMSAs. Lanes as well as free and shifted bands were added and adjusted manually, and pixel intensity values were reported as band percentage. For dsDNA EMSAs, free dsDNA band percentages were normalized to the probe only control band percentage. The free DNA band percentage values were then used to determine the percent shifted of the respective probe relative to the free probe. For RNA and ssDNA EMSAs, lanes and bands were selected manually, and the shifted bands were analyzed to obtain the percent shifted values. Background and any ssDNA probe percentage that was shifted were subtracted from the percent totals. For competition EMSAs, the band intensity values of each band in a lane were determined manually using the lane profile tool. The amount of free probe in the experimental lanes was normalized to the probe only control band percentage value. Any probe signal stuck in the gel wells, attributed to potential protein aggregation, were not considered shifts, and thus omitted from densitometric analysis.

To calculate the apparent dissociation constant ( $K_D$ ), nonlinear regression analysis was performed to determine the best-fit

values for each experimental condition tested. Briefly, protein concentrations were plotted against the shifted band percentage values obtained from densitometry using the one-site specific binding setting in Prism GraphPad 9.5.1. Confidence was set at 95% with the analysis considering each replicate value from triplicate EMSAs performed for the analysis. Either a Welch's t-test or Welch ANOVA followed by a Dunnett's T3 multiple comparisons test, was used to compare fits.

#### 4.8 | Major and minor groove binding assay

The IRDye 800 labeled *glpFKD(-7/+35)* DNA probe was used in the major and minor groove binding assay. The reactions were assembled similarly to the EMSA reactions described above. Briefly, 2.5  $\mu$ M of WT PlzA was incubated with 100  $\mu$ M c-di-GMP in EMSA buffer for 5 minutes. The *glpFKD(-7/+35)* DNA probe (10 nM) was then added to the reaction mixture which was allowed to incubate for an additional 10 minutes at room temperature. After the probe incubation, 0.25–250  $\mu$ M of either methyl green (major groove binder) or actinomycin D (minor groove binder) were added to the reaction mixture and allowed to incubate for 5 minutes at room temperature. EMSA loading dye (0.8 mg/mL Orange G, 15 mg/mL Ficoll 400) was added to each reaction, and the reaction mixtures were subsequently loaded onto pre-run 10% Novex TBE gels. Gels were resolved and images acquired as described above for EMSAs.

#### 4.9 | Docking analysis and protein modeling

Computational modeling of holo-PlzA (PDB ID: 7mie) in complex with the nucleic acids of interest was performed using the HDock server: <http://hdock.phys.hust.edu.cn/>. Briefly, the PDB and chain ID of PlzA was entered for the input receptor molecule to retrieve the crystal structure of the protein for the analysis. For each analysis, the corresponding nucleic acid sequence of interest was then pasted as the input ligand molecule, and the type of nucleic acid selected from the drop-down menu. The input nucleic acid sequences are listed in Table 2. All analyses were performed with default parameters. The top model for each computation is shown. Docking and confidence scores are provided in the corresponding figure legends. The more negative the docking score, the more probable the binding. A confidence score above 0.7 indicates the molecules would be highly likely to bind.

Protein structure prediction for PlzA<sub>NTD</sub>, PlzA<sub>CTD</sub>, and PlzA<sub>RD-RD</sub> was performed via AlphaFold. All output PDB files generated from the various analyses were viewed with ChimeraX 1.4 (Goddard et al., 2018; Jumper et al., 2021; Pettersen et al., 2021).

#### 4.10 | Cyclic di-nucleotide LC-MS analysis

Detection of cyclic di-nucleotides in recombinant protein purifications was conducted by liquid chromatography–tandem mass

spectrometry (LC-MS/MS) at the Michigan State University Mass Spectrometry core. Briefly, recombinant proteins were purified and quantified as mentioned previously and subsequently dialyzed into EMSA buffer without Tween-20. For LC-MS/MS analysis, approximately 1 mg/mL of PlzA<sub>WT</sub>, PlzA<sub>RD-RD</sub>, PlzA<sub>NTD</sub>, and PlzA<sub>CTD</sub> were aliquoted and stored at  $-80^{\circ}\text{C}$  until shipment to the core facility. Nucleotides bound to purified protein samples (1 mg/mL) were analyzed by precipitating protein with 3 volumes of acetonitrile followed by centrifugation to pellet precipitated protein. The supernatant was transferred to a new tube and evaporated to dryness. The sample was reconstituted in mobile phase solvent A (10 mM tributylamine +15 mM acetic acid in water/methanol, 97:3 v/v). LC-MS analysis was performed on a Waters Xevo G2-XS Quadrupole-Time-of-Flight (QToF) mass spectrometer interfaced with a Waters Acquity UPLC system. 10  $\mu$ L of sample was injected onto a Waters Acquity BEH-C18 UPLC column (2.1  $\times$  50 mm) and compounds were separated using the following gradient: initial conditions were 100% mobile phase A, hold at 100% A until 1 min, ramp to 99% B at 7 min (mobile phase B: methanol), hold at 99% B until 8 min, return to 100% A at 8.01 min and hold until 10 min. The flow rate through the column was 0.3 mL/min and the column temperature was held at 40  $^{\circ}\text{C}$ . Compounds were ionized by electrospray ionization operated in negative mode. Capillary voltage was 2.0 kV, cone voltage was 35, source temperature was 100  $^{\circ}\text{C}$  and desolvation temperature was 350  $^{\circ}\text{C}$ . The cone gas and desolvation gas flows were 50 L/hr and 600 L/hr respectively. A TOF MS scan method with targeted enhancement of m/z 689 was used with 0.5 second scan time. Lockmass correction was performed using leucine enkephalin as the reference compound.

Data were processed using Waters Masslynx software. Extracted ion chromatograms were performed to look for the presence of c-di-GMP (m/z 689.09), c-di-AMP (m/z 657.09) and c-GAMP (673.09). The intensity values were converted to relative abundance as determined from the base peak values. The c-di-GMP concentration was determined from the peak area of the target compound against a standard curve of known c-di-GMP concentrations. These concentrations were calculated using the Targetlynx tool in the Waters Masslynx software. The percentage of protein bound with c-di-GMP was calculated from the total protein and calculated c-di-GMP concentrations in each sample.

#### 4.11 | Circular dichroism spectroscopy

The CD analysis was performed at the University of Kentucky Center for Molecular Medicine Protein Core. Briefly, proteins were either buffer exchanged or diluted into 10 mM sodium phosphate buffer, pH 7.0. A 400  $\mu$ L solution of each protein at a concentration of 100  $\mu$ g/mL was pipetted into a 1 mm quartz cuvette and loaded into a Jasco J-810 spectrophotometer. The samples were scanned at 0.1 nm increments and CD spectra collected for wavelengths 185–260 nm with the temperature held constant at 25  $^{\circ}\text{C}$ . A buffer only sample was used as a control. Two independent recombinant

protein preparations were analyzed for each protein type. Spectral data was deconvoluted using CDtoolX. Deconvolution consisted of buffer spectra subtraction and the conversion of the CD spectra to molar residue ellipticity to normalize the data for sample concentration and sequence length. Data were visualized in GraphPad Prism 10.1.2.

Secondary structure prediction was performed using the BeStSel webserver using the single spectrum analysis function (Micsonai et al., 2015, 2018, 2022). Mean residue ellipticity values from the deconvoluted CD data were input into the server for analysis. The PDB file, 7MIE, was used to determine the secondary structure of the crystallized PlzA protein for comparisons to the generated recombinant proteins.

## AVAILABILITY

HDOCK (<http://hdock.phys.hust.edu.cn/>).

CDtoolX (<https://cdtools.cryst.bbk.ac.uk/>).

BeStSel (<https://bestsel.elte.hu/index.php>).

## AUTHOR CONTRIBUTIONS

**Brian Stevenson:** Conceptualization; funding acquisition; writing – review and editing; supervision; project administration. **Nerina Jusufovic:** Conceptualization; investigation; writing – original draft; methodology; validation; visualization; writing – review and editing; formal analysis; data curation. **Andrew C. Krusenstjerna:** Conceptualization; investigation; writing – review and editing. **Christina R. Savage:** Conceptualization; investigation; writing – review and editing. **Timothy C. Saylor:** Conceptualization; methodology; writing – review and editing. **Catherine Brissette:** Conceptualization; writing – review and editing; funding acquisition. **Wolfram R. Zückert:** Conceptualization; funding acquisition; writing – review and editing. **Paula J. Schlax:** Conceptualization; funding acquisition; writing – review and editing; methodology; resources. **Md A. Motaleb:** Conceptualization; funding acquisition; investigation; resources; writing – review and editing.

## ACKNOWLEDGEMENTS

We dedicate this manuscript to our friend and colleague Christina R. Savage, Ph.D., whose initial studies on PlzA were invaluable to this work. We also thank Jessamyn Morris and Tatiana Castro Padovani for their support of the studies undertaken. Circular Dichroism was performed at the University of Kentucky Center for Molecular Medicine, and we thank Martin Chow for his assistance on these studies. The LC-MS/MS to detect di-nucleotides was performed by the Mass Spectrometry and Metabolomics Core at Michigan State University. A sincere thank you to Tony Schillmiller at MSU for all his help with the mass spectrometry services. Figures 1, 4a, 6a, 7a, 10a, and 13 were created via BioRender. Lastly, we thank Dr. József Kardos at Eötvös Loránd University for providing the secondary structure analysis for the 7MIE PDB file via email. Funding for open access charge: US National Institutes of Health (grant R01 AI144126-3 to B.S.).

## CONFLICT OF INTEREST STATEMENT

None declared.

## DATA AVAILABILITY STATEMENT

The data that support the findings of this study are available from the corresponding author upon reasonable request.

## ETHICS STATEMENT

No human or animal subjects were used in this study.

## ORCID

Wolfram R. Zückert  <https://orcid.org/0000-0002-7350-2162>

Md A. Motaleb  <https://orcid.org/0000-0003-2761-5104>

Brian Stevenson  <https://orcid.org/0000-0002-2406-4776>

## REFERENCES

- Adams, P.P., Avile, C.F., Popitsch, N., Bilusic, I., Schroeder, R., Lybecker, M. et al. (2017) In vivo expression technology and 5' end mapping of the *Borrelia burgdorferi* transcriptome identify novel RNAs expressed during mammalian infection. *Nucleic Acids Research*, 45, 775–792.
- Amikam, D. & Galperin, M.Y. (2006) PilZ domain is part of the bacterial c-di-GMP binding protein. *Bioinformatics*, 22, 3–6. Available from: <https://academic.oup.com/bioinformatics/article/22/1/3/218448> [Accessed 18th February 2022].
- Babb, K., Bykowski, T., Riley, S.P., Miller, M.C., Demoll, E. & Stevenson, B. (2006) *Borrelia burgdorferi* EbfC, a novel, chromosomally encoded protein, binds specific DNA sequences adjacent to *erp* loci on the spirochete's resident cp32 prophages. *Journal of Bacteriology*, 188, 4331–4339. Available from: <https://journals.asm.org/journal/jb> [Accessed 8th April 2022].
- Basu, D., Khare, G., Singh, S., Tyagi, A., Khosla, S. & Mande, S.C. (2009) A novel nucleoid-associated protein of mycobacterium tuberculosis is a sequence homolog of GroEL. *Nucleic Acids Research*, 37, 4944–4954.
- Bauer, W.J., Luthra, A., Zhu, G., Radolf, J.D., Malkowski, M.G. & Caimano, M.J. (2015) Structural characterization and modeling of the *Borrelia burgdorferi* hybrid histidine kinase Hk1 periplasmic sensor: a system for sensing small molecules associated with tick feeding. *Journal of Structural Biology*, 192, 48–58.
- Bong, H.J., Ko, E.M., Song, S.Y., Ko, I.J. & Oh, J.I. (2019) Tripartite regulation of the *glpFKD* operon involved in glycerol catabolism by *gylr*, *crp*, and *sigf* in *Mycobacterium smegmatis*. *Journal of Bacteriology*, 201, e00511-19.
- Burns, L.H., Adams, C.A., Riley, S.P., Jutras, B.L., Bowman, A., Chenail, A.M. et al. (2010) BpaB, a novel protein encoded by the Lyme disease spirochete's cp32 prophages, binds to *erp* operator 2 DNA. *Nucleic Acids Research*, 38, 5443–5455.
- Caimano, M.J., Dunham-Ems, S., Allard, A.M., Cassera, M.B., Kenedy, M. & Radolf, J.D. (2015) Cyclic di-GMP modulates gene expression in Lyme disease spirochetes at the tick-mammal interface to promote spirochete survival during the blood meal and tick-to-mammal transmission. *Infection and Immunity*, 83, 3043–3060. Available from: <https://doi.org/10.1128/IAI.00315-15>
- Caimano, M.J., Kenedy, M.R., Kairu, T., Desrosiers, D.C., Harman, M., Dunham-Ems, S. et al. (2011) The hybrid histidine kinase Hk1 is part of a two-component system that is essential for survival of *Borrelia burgdorferi* in feeding *Ixodes scapularis* ticks. *Infection and Immunity*, 79, 3117–3130. Available from: <http://www.ncbi.nlm.nih.gov/Structure/cdd/cdd.shtml> [Accessed 13th February 2022].

- Carey, J. (2022) Affinity, specificity, and cooperativity of DNA binding by bacterial gene regulatory proteins. *International Journal of Molecular Sciences*, 23, 1–16.
- Casjens, S., Palmer, N., Van Vugt, R., Huang, W.M., Stevenson, B., Rosa, P. et al. (2000) A bacterial genome in flux: the twelve linear and nine circular extrachromosomal DNAs in an infectious isolate of the Lyme disease spirochete *Borrelia burgdorferi*. *Molecular Microbiology*, 35, 490–516.
- Cheang, Q.W., Xin, L., Chea, R.Y.F. & Liang, Z.X. (2019) Emerging paradigms for PilZ domain-mediated c-di-GMP signaling. *Biochemical Society Transactions*, 47, 381–388.
- Chou, S.H. & Galperin, M.Y. (2016) Diversity of cyclic di-GMP-binding proteins and mechanisms. *Journal of Bacteriology*, 198, 32–46. Available from: [http://ncbi.nlm.nih.gov/Complete\\_Genomes/c-di-GMP.html](http://ncbi.nlm.nih.gov/Complete_Genomes/c-di-GMP.html) [Accessed 13th February 2022].
- Corona, A. & Schwartz, I. (2015) *Borrelia burgdorferi*: carbon metabolism and the tick-mammal enzootic cycle. *Microbiology Spectrum*, 3. Available from: <https://doi.org/10.1128/microbiolspec.MBP-0011-2014>
- Fraser, C.M., Casjens, S., Huang, W.M., Sutton, G.G., Clayton, R., Lathigra, R. et al. (1997) Genomic sequence of a Lyme disease spirochaete, *Borrelia burgdorferi*. *Nature*, 390, 580–586.
- Freedman, J.C., Rogers, E.A., Kostick, J.L., Zhang, H., Iyer, R., Schwartz, I. et al. (2009) Identification and molecular characterization of a cyclic-di-GMP effector protein, PlzA (BB0733): additional evidence for the existence of a functional cyclic-di-GMP regulatory network in the Lyme disease spirochete, *Borrelia burgdorferi*. *FEMS Immunology and Medical Microbiology*, 58, 285–294. Available from: <https://academic.oup.com/femspd/article/58/2/285/597665> [Accessed 26th April 2021].
- Fried, M. & Crothers, D.M. (1981) Equilibria and kinetics of lac repressor-operator interactions by polyacrylamide gel electrophoresis. *Nucleic Acids Research*, 9, 1981–6525.
- Fried, M.G. (1989) Measurement of protein-DNA interaction parameters by electrophoresis mobility shift assay. *Electrophoresis*, 10, 366–376.
- Galperin, M.Y. & Chou, S.H. (2020) Structural conservation and diversity of PilZ-related domains. *Journal of Bacteriology*, 202. Available from: <https://doi.org/10.1128/jb.00664-19>
- Galperin, M.Y., Nikolskaya, A.N. & Koonin, E.V. (2001) Novel domains of the prokaryotic two-component signal transduction systems. *FEMS Microbiology Letters*, 203, 11–21. Available from: <https://academic.oup.com/femsls/article/203/1/11/478433> [Accessed 17th March 2022].
- Goddard, T.D., Huang, C.C., Meng, E.C., Pettersen, E.F., Couch, G.S., Morris, J.H. et al. (2018) UCSF ChimeraX: meeting modern challenges in visualization and analysis. *Protein Science*, 27, 14–25.
- Grassmann, A.A., Tokarz, R., Golino, C., McLain, M.A., Groshong, A.M., Radolf, J.D. et al. (2023) BosR and PlzA reciprocally regulate RpoS function to sustain *Borrelia burgdorferi* in ticks and mammals. *Journal of Clinical Investigation*, 133, e166710. Available from: <http://www.jci.org/articles/view/166710>
- Groshong, A.M., Grassmann, A.A., Luthra, A., McLain, M.A., Provas, A.A., Radolf, J.D. et al. (2021) PlzA is a bifunctional c-di-GMP biosensor that promotes tick and mammalian host-adaptation of *Borrelia burgdorferi*. *PLoS Pathogens*, 17, 1–31.
- Grove, A.P., Liveris, D., Iyer, R., Petzke, M., Rudman, J., Caimano, M.J. et al. (2017) Two distinct mechanisms govern RpoS-mediated repression of tick-phase genes during mammalian host adaptation by *Borrelia burgdorferi*, the Lyme disease spirochete. *MBio*, 8, e01204-17. Available from: <https://doi.org/10.1128/mBio.01204-17>
- He, M., Ouyang, Z., Troxell, B., Xu, H., Moh, A., Piesman, J. et al. (2011) Cyclic di-gmp is essential for the survival of the Lyme disease spirochete in ticks. *PLoS Pathogens*, 7, e1002133.
- He, M., Zhang, J.J., Ye, M., Lou, Y. & Yang, X.F. (2014) Cyclic Di-GMP receptor PlzA controls virulence gene expression through RpoS in *Borrelia burgdorferi*. *Infection and Immunity*, 82, 445–452. Available from: <http://iai.asm.org/> [Accessed 26th April 2021].
- Helble, J.D., McCarthy, J.E. & Hu, L.T. (2021) Interactions between *Borrelia burgdorferi* and its hosts across the enzootic cycle. *Parasite Immunology*, 43, e12816.
- Hellman, L.M. & Fried, M.G. (2007) Electrophoretic mobility shift assay (EMSA) for detecting protein-nucleic acid interactions. *Nature Protocols*, 2, 1849–1861.
- Hengge, R. (2009) Principles of c-di-GMP signalling in bacteria. *Nature Reviews. Microbiology*, 7, 263–273.
- Hsieh, M.L., Hinton, D.M. & Waters, C.M. (2018) VpsR and cyclic di-GMP together drive transcription initiation to activate biofilm formation in *Vibrio cholerae*. *Nucleic Acids Research*, 46, 8876–8887.
- Huang, S.Y. & Zou, X. (2014) A knowledge-based scoring function for protein-RNA interactions derived from a statistical mechanics-based iterative method. *Nucleic Acids Research*, 42, e55.
- Jenal, U., Reinders, A. & Lori, C. (2017) Cyclic di-GMP: second messenger extraordinaire. *Nature Reviews. Microbiology*, 15, 271–284. Available from: <https://doi.org/10.1038/nrmicro.2016.190>
- Jumper, J., Evans, R., Pritzel, A., Green, T., Figurnov, M., Ronneberger, O. et al. (2021) Highly accurate protein structure prediction with AlphaFold. *Nature*, 596, 583–589. Available from: <https://doi.org/10.1038/s41586-021-03819-2>
- Junkermeier, E.H. & Hengge, R. (2023) Local signaling enhances output specificity of bacterial c-di-GMP signaling networks. *microLife*, 4, uqad026.
- Jutras, B.L., Bowman, A., Brissette, C.A., Adams, C.A., Verma, A., Chenail, A.M. et al. (2012) EbfC (YbaB) is a new type of bacterial nucleoid-associated protein and a global regulator of gene expression in the Lyme disease spirochete. *Journal of Bacteriology*, 194, 3395–3406.
- Jutras, B.L., Chenail, A.M., Carroll, D.W., Miller, M.C., Zhu, H., Bowman, A. et al. (2013) Bpur, the Lyme disease spirochete's PUR domain protein: identification as a transcriptional modulator and characterization of nucleic acid interactions. *Journal of Biological Chemistry*, 288, 26220–26234. Available from: <http://www.jbc.org/> [Accessed 5th October 2020].
- Jutras, B.L., Chenail, A.M., Rowland, C.L., Carroll, D., Miller, M.C., Bykowski, T. et al. (2013) Eubacterial SpoVG homologs constitute a new family of site-specific DNA-binding proteins. *PLoS One*, 8, 66683.
- Kim, B. & Little, J.W. (1992) Dimerization of a specific DNA-binding protein on the DNA. *Science*, 255, 203–206.
- Kim, S.K. & Nordén, B. (1993) Methyl green. A DNA major-groove binding drug. *FEBS Letters*, 315, 61–64.
- Kohler, J.J., Metallo, S.J., Schneider, T.L. & Schepartz, A. (1999) DNA specificity enhanced by sequential binding of protein monomers. *Proceedings of the National Academy of Sciences of the United States of America*, 96, 11735–11739.
- Kostick, J.L., Szkotnicki, L.T., Rogers, E.A., Bocci, P., Raffaelli, N. & Marconi, R.T. (2011) The diguanylate cyclase, Rrp1, regulates critical steps in the enzootic cycle of the Lyme disease spirochetes. *Molecular Microbiology*, 81, 219–231. Available from: <https://doi.org/10.1111/j.1365-2958.2011.07687.x>
- Kostick-Dunn, J.L., Izac, J.R., Freedman, J.C., Szkotnicki, L.T., Oliver, L.D. & Marconi, R.T. (2018) The *Borrelia burgdorferi* c-di-GMP binding receptors, PlzA and PlzB, are functionally distinct. *Frontiers in Cellular and Infection Microbiology*, 8, 213.
- Krusenstjerna, A.C., Arnold, W.K., Saylor, T.C., Tucker, J.S. & Stevenson, B. (2023) *Borrelia burgdorferi* DnaA and the nucleoid-associated protein EbfC coordinate expression of the *dnaX-ebfC* operon. *Journal of Bacteriology*, 205, e00396-22. Available from: <https://doi.org/10.1128/jb.00396-22>

- Larouche, K., Bergeron, M.-J., Leclerc, S. & Guerin, S. (1996) Optimization of competitor poly(dI-dC). Poly(dI-dC) levels is advised in DNA-protein interaction studies involving enriched nuclear proteins. *BioTechniques*, 20, 439–444.
- Lee, R.E. & Baust, J.G. (1987) Cold-hardiness in the Antarctic tick, *Ixodes uriae*. *Physiological Zoology*, 60, 499–506. Available from: <https://about.jstor.org/terms>
- Liu, Y., Wang, H., Cui, T., Zhou, X., Jia, Y., Zhang, H. et al. (2016) NapM, a new nucleoid-associated protein, broadly regulates gene expression and affects mycobacterial resistance to anti-tuberculosis drugs. *Molecular Microbiology*, 101, 167–181.
- Mallory, K.L., Miller, D.P., Oliver, L.D., Freedman, J.C., Kostick-Dunn, J.L., Carlyon, J.A. et al. (2016) Cyclic-di-GMP binding induces structural rearrangements in the PlzA and PlzC proteins of the Lyme disease and relapsing fever spirochetes: a possible switch mechanism for c-di-GMP-mediated effector functions. *Pathogens and Disease*, 74, 1–8.
- Micsonai, A., Moussong, É., Wien, F., Boros, E., Vadász, H., Murvai, N. et al. (2022) BeStSel: webserver for secondary structure and fold prediction for protein CD spectroscopy. *Nucleic Acids Research*, 50, W90–W98.
- Micsonai, A., Wien, F., Bulyáki, É., Kun, J., Moussong, É., Lee, Y.H. et al. (2018) BeStSel: a web server for accurate protein secondary structure prediction and fold recognition from the circular dichroism spectra. *Nucleic Acids Research*, 46, W315–W322.
- Micsonai, A., Wien, F., Kernya, L., Lee, Y.H., Goto, Y., Réfrégiers, M. et al. (2015) Accurate secondary structure prediction and fold recognition for circular dichroism spectroscopy. *Proceedings of the National Academy of Sciences of the United States of America*, 112, E3095–E3103.
- Novak, E.A., Sultan, S.Z. & Motaleb, M.A. (2014) The cyclic-di-GMP signaling pathway in the Lyme disease spirochete, *Borrelia burgdorferi*. *Frontiers in Cellular and Infection Microbiology*, 4, 56.
- Pappas, C.J., Iyer, R., Petzke, M.M., Caimano, M.J., Radolf, J.D. & Schwartz, I. (2011) *Borrelia burgdorferi* requires glycerol for maximum fitness during the tick phase of the enzootic cycle. *PLoS Pathogens*, 7, e1002102.
- Pettersen, E.F., Goddard, T.D., Huang, C.C., Meng, E.C., Couch, G.S., Croll, T.I. et al. (2021) UCSF ChimeraX: structure visualization for researchers, educators, and developers. *Protein Science*, 30, 70–82.
- Pitzer, J.E., Syed, S.Z., Hayakawa, Y., Hobbs, G., Miller, M.R. & Motaleb, M.A. (2011) Analysis of the *Borrelia burgdorferi* cyclic-di-GMP-binding protein PlzA reveals a role in motility and virulence. *Infection and Immunity*, 79, 1815–1825. Available from: <http://iaiasm.org/> [Accessed 26th April 2021].
- Pronobis, M.I., Deutch, N. & Peifer, M. (2016) The Miraprep: a protocol that uses a Miniprep kit and provides Maxiprep yields. *PLoS One*, 11, 1–12.
- Pultz, I.S., Christen, M., Kulasekara, H.D., Kennard, A., Kulasekara, B. & Miller, S.I. (2012) The response threshold of salmonella PilZ domain proteins is determined by their binding affinities for c-di-GMP. *Molecular Microbiology*, 86, 1424–1440.
- Riley, S.P., Bykowski, T., Cooley, A.E., Burns, L.H., Babb, K., Brissette, C.A. et al. (2009) *Borrelia burgdorferi* EbfC defines a newly-identified, widespread family of bacterial DNA-binding proteins. *Nucleic Acids Research*, 37, 1973–1983. Available from: <http://www.rcsb.org/> [Accessed 8th April 2022].
- Rogers, E.A., Terekhova, D., Zhang, H.-M.M., Hovis, K.M., Schwartz, I. & Marconi, R.T. (2009) Rrp1, a cyclic-di-GMP-producing response regulator, is an important regulator of *Borrelia burgdorferi* core cellular functions. *Molecular Microbiology*, 71, 1551–1573. Available from: <http://www.pubmedcentral.nih.gov/articlerender.fcgi?artid=2843504&tool=pmcentrez&rendertype=abstract> [Accessed 18th February 2022].
- Romling, U., Galperin, M.Y. & Gomelsky, M. (2013) Cyclic di-GMP: the first 25 years of a universal bacterial second messenger. *Microbiology and Molecular Biology Reviews*, 77, 1–52.
- Rooman, M., Lié Vin, J., Buisine, E. & Wintjens, R. (2002) Cation-p/H-bond stair motifs at protein-DNA interfaces. *Journal of Molecular Biology*, 319, 67–76. Available from: <http://www.idealibrary.com>
- Ryjenkov, D.A., Simm, R., Römling, U. & Gomelsky, M. (2006) The PilZ domain is a receptor for the second messenger c-di-GMP: the PilZ domain protein YcgR controls motility in enterobacteria. *Journal of Biological Chemistry*, 281, 30310–30314.
- Ryjenkov, D.A., Tarutina, M., Moskvina, O.V. & Gomelsky, M. (2005) Cyclic diguanylate is a ubiquitous signaling molecule in bacteria: insights into biochemistry of the GGDEF protein domain. *Journal of Bacteriology*, 187, 1792–1798. Available from: <https://doi.org/10.1128/JB.187.5.1792-1798.2005>
- Sarenko, O., Klaucek, G., Wilke, F.M., Pfiffer, V., Richter, A.M., Herbst, S. et al. (2017) More than enzymes that make or break cyclic Di-GMP—local signaling in the interactome of GGDEF/EAL domain proteins of *Escherichia coli*. *MBio*, 8, e01639-17.
- Sathyapriya, R. & Vishveshwara, S. (2004) Interaction of DNA with clusters of amino acids in proteins. *Nucleic Acids Research*, 32, 4109–4118.
- Savage, C.R., Jutras, B.L., Bestor, A., Tilly, K., Rosa, P.A., Tourand, Y. et al. (2018) *Borrelia burgdorferi* SpoVG DNA- and RNA-binding protein modulates the physiology of the Lyme disease spirochete. *Journal of Bacteriology*, 200, e00033-18. Available from: <http://jb.asm.org/> [Accessed 26th April 2021].
- Saylor, T.C., Savage, C.R., Krusenstjerna, A.C., Jusufovic, N., Zückert, W.R., Brissette, C.A. et al. (2023) Quantitative analyses of interactions between SpoVG and RNA/DNA. *Biochemical and Biophysical Research Communications*, 654, 40–46.
- Schäper, S., Steinchen, W., Krol, E., Altegoer, F., Skotnicka, D., Søgaard-Andersen, L. et al. (2017) AraC-like transcriptional activator CuxR binds c-di-GMP by a PilZ-like mechanism to regulate extracellular polysaccharide production. *Proceedings of the National Academy of Sciences of the United States of America*, 114, E4822–E4831.
- Schramm, F.D., Schroeder, K. & Jonas, K. (2019) Protein aggregation in bacteria. *FEMS Microbiology Reviews*, 44, 54–72.
- Shi, W.T., Zhang, B., Li, M.L., Liu, K.H., Jiao, J. & Tian, C.F. (2022) The convergent xenogeneic silencer MucR predisposes  $\alpha$ -proteobacteria to integrate AT-rich symbiosis genes. *Nucleic Acids Research*, 50, 8580–8598.
- Singh, A., Izac, J.R., Schuler, E.J.A., Patel, D.T., Davies, C. & Marconi, R.T. (2021) High-resolution crystal structure of the *Borrelia burgdorferi* PlzA protein in complex with c-di-GMP: new insights into the interaction of c-di-GMP with the novel xPilZ domain. *Pathogens and Disease*, 79, 1–9.
- Skotnicka, D., Steinchen, W., Szadkowski, D., Cadby, I.T., Lovering, A.L., Bange, G. et al. (2020) CdbA is a DNA-binding protein and c-di-GMP receptor important for nucleoid organization and segregation in *Myxococcus xanthus*. *Nature Communications*, 11, 1791. Available from: <https://doi.org/10.1038/s41467-020-15628-8>
- Sultan, S.Z., Pitzer, J.E., Boquoi, T., Hobbs, G., Miller, M.R. & Motaleb, M.A. (2011) Analysis of the HD-GYP domain cyclic dimeric gmp phosphodiesterase reveals a role in motility and the enzootic life cycle of *Borrelia burgdorferi*. *Infection and Immunity*, 79, 3273–3283.
- Sultan, S.Z., Pitzer, J.E., Miller, M.R. & Motaleb, M.A. (2010) Analysis of a *Borrelia burgdorferi* phosphodiesterase demonstrates a role for cyclic-di-guanosine monophosphate in motility and virulence. *Molecular Microbiology*, 77, 128–142.
- Tan, J.W.H., Wilksch, J.J., Hocking, D.M., Wang, N., Srihanta, Y.N., Tauschek, M. et al. (2015) Positive autoregulation of *mrkHI* by the cyclic Di-GMP-dependent MrkH protein in the biofilm regulatory circuit of *Klebsiella pneumoniae*. *Journal of Bacteriology*, 197, 1659–1667.
- Tschowri, N., Schumacher, M.A., Schlimpert, S., Chinnam, N.B., Findlay, K.C., Brennan, R.G. et al. (2014) Tetrameric c-di-GMP mediates effective transcription factor dimerization to control *Streptomyces* development. *Cell*, 158, 1136–1147. Available from: <https://doi.org/10.1016/j.cell.2014.07.022>

- Valentini, M. & Filloux, A. (2019) Multiple roles of c-di-GMP signaling in bacterial pathogenesis. *Annual Review of Microbiology*, 73, 387–406.
- Van Gundy, T., Patel, D., Bowler, B.E., Rothfuss, M.T., Hall, A.J., Davies, C. et al. (2023) c-di-GMP regulates activity of the PlzA RNA chaperone from the Lyme disease spirochete. *Molecular Microbiology*, 119, 711–727.
- Wang, F., He, Q., Su, K., Gao, F., Huang, Y., Lin, Z. et al. (2016) The PilZ domain of MrkH represents a novel DNA binding motif. *Protein & Cell*, 7, 766–772. Available from: <https://www.ncbi.nlm.nih.gov/pmc/articles/PMC5055493/> [Accessed 13th February 2022].
- Wilksch, J.J., Yang, J., Clements, A., Gabbe, J.L., Short, K.R., Cao, H. et al. (2011) MrkH, a novel c-di-GMP-dependent transcriptional activator, controls *Klebsiella pneumoniae* biofilm formation by regulating type 3 fimbriae expression. *PLoS Pathogens*, 7, e1002204. Available from: <https://doi.org/10.1371/journal.ppat.1002204>
- Yan, Y., Tao, H., He, J. & Huang, S.Y. (2020) The HDock server for integrated protein–protein docking. *Nature Protocols*, 15, 1829–1852.
- Yan, Y., Wen, Z., Wang, X. & Huang, S.Y. (2017) Addressing recent docking challenges: a hybrid strategy to integrate template-based and free protein–protein docking. *Proteins: Structure, Function, and Bioinformatics*, 85, 497–512.
- Yan, Y., Zhang, D., Zhou, P., Li, B. & Huang, S.Y. (2017) HDock: a web server for protein–protein and protein–DNA/RNA docking based on a hybrid strategy. *Nucleic Acids Research*, 45, W365–W373.
- Yang, J., Wilksch, J.J., Tan, J.W.H., Hocking, D.M., Webb, C.T., Lithgow, T. et al. (2013) Transcriptional activation of the *mrkA* promoter of the *Klebsiella pneumoniae* type 3 fimbrial operon by the c-di-GMP-dependent MrkH protein. *PLoS One*, 8, e79038.
- Zamorano-Sánchez, D., Fong, J.C.N., Kilic, S., Erill, I. & Yildiz, F.H. (2015) Identification and characterization of VpsR and VpsT binding sites in *Vibrio cholerae*. *Journal of Bacteriology*, 197, 1221–1235. Available from: <https://doi.org/10.1128/JB.02439-14>
- Zhang, J.J., Chen, T., Yang, Y., Du, J., Li, H., Troxell, B. et al. (2018) Positive and negative regulation of glycerol utilization by the c-di-GMP binding protein PlzA in *Borrelia burgdorferi*. *Journal of Bacteriology*, 200, e00243-18. Available from: <https://doi.org/10.1128/JB.00243-18>
- Zhang, J.-J., Raghunandan, S., Wang, Q., Priya, R., Alanazi, F., Lou, Y. et al. (2024) BadR directly represses the expression of the glycerol utilization operon in the Lyme disease pathogen. *Journal of Bacteriology*, 206, e0034023. Available from: <https://doi.org/10.1128/jb.00340-23>

## SUPPORTING INFORMATION

Additional supporting information can be found online in the Supporting Information section at the end of this article.

**How to cite this article:** Jusufovic, N., Krusenstjerna, A.C., Savage, C.R., Saylor, T.C., Brissette, C.A., Zückert, W.R. et al. (2024) *Borrelia burgdorferi* PlzA is a cyclic-di-GMP dependent DNA and RNA binding protein. *Molecular Microbiology*, 121, 1039–1062. Available from: <https://doi.org/10.1111/mmi.15254>